

AN IN VITRO STUDY OF THE P53 PROTEIN FAMILY AND ITS  
INTERACTION WITH HUMAN PAPILLOMAVIRUS PROTEIN E6

MICHAEL T. PINNER



A thesis submitted for the degree of Master of Science (Diplom-Ingenieur)  
at the University of Natural Resources and Life Sciences, Vienna

April 2017

SUPERVISORS

Prof. Xin Lu (University of Oxford)

Prof. Johannes Grillari (University of Natural Resources and Life Sciences, Vienna)

Michael T. Pinner: *An in vitro study of the p53 protein family and its interaction with human papillomavirus protein E6*, A thesis submitted for the degree of Master of Science (Diplom-Ingenieur), © April 2017

SUPERVISORS:

Prof. Xin Lu

Ludwig Institute for Cancer Research, University of Oxford

Prof. Johannes Grillari

Department of Biotechnology, University of Natural Resources and Life Sciences, Vienna

## ABSTRACT

---

The tumour suppressor p53 is the most commonly inactivated protein in cancer. It plays a central role in the DNA damage response and has therefore been dubbed 'guardian of the genome'. Along with its sister proteins p63 and p73, p53 forms the heavily researched p53 protein family. The importance of p53 becomes evident in cervical carcinoma, which can be traced back to an infection with high-risk types of human papillomavirus (HPV) in nearly every case. An essential mechanism in the carcinogenesis of cervical carcinoma is the rapid degradation of p53 by the viral protein E6 in HPV infected cells. Despite their structural similarity to p53 there is only limited data regarding the susceptibility of p63 and p73 to E6 mediated degradation. Due to the particularity of p63 and p73 to be produced as several variants (isoforms) with different properties, further investigations of both proteins are considerably more complex. In this master's thesis it is shown that E6 targets all tested isoforms of p63 and p73 for degradation in vitro, although this process is considerably less efficient than for p53. The degradation of p53 under different conditions is also discussed. Finally it is shown that following in vitro transcription and translation in presence of the oxygenase inhibitor N-Oxalylglycine, p53 and 18E6 are detectable at elevated levels.

## ZUSAMMENFASSUNG

---

Der Tumorsuppressor p53 ist das am häufigsten inaktivierte Protein in Krebstumoren. Er spielt eine wesentliche Rolle in der Reaktion auf DNA-Schäden und wird aufgrund seiner Bedeutung auch als „Wächter des Genoms“ bezeichnet. Zusammen mit seinen Schwesterproteinen p63 und p73 bildet p53 eine Proteinfamilie, welche Gegenstand intensiver Forschungsbemühungen ist. Die Wichtigkeit von p53 verdeutlicht sich unter anderem im Zervixkarzinom, dessen Entstehung in nahezu jedem Fall auf eine Infektion mit Hochrisiko-Typen des Humanen Papillomvirus (HPV) zurückgeführt werden kann. Ein wesentlicher Mechanismus hierbei ist der rasche Abbau des Tumorsuppressorproteins p53 durch das virale Protein E6 in von HPV infizierten Zellen. Trotz ihrer strukturellen Ähnlichkeit zu p53 gibt es allerdings nur wenige Studien bezüglich der Anfälligkeit von p63 und p73 für einen Abbau durch E6. Zudem wird eine Datenerhebung dadurch verkompliziert, dass von beiden Proteinen mehrere Varianten (Isoformen) mit unterschiedlichen Eigenschaften gebildet werden können. In dieser Masterarbeit wird gezeigt, dass E6 den Abbau sämtlicher getesteter Isoformen von p63 und p73 fördert, und dass dieser Prozess ineffizienter ist als bei p53. Der Abbau von p53 unter verschiedenen Bedingungen wird ebenfalls diskutiert. Abschließend wird beschrieben, dass p53 und E6 nach in vitro Transkription und Translation in Anwesenheit des Oxygenaseinhibitors N-Oxalylglycin in erhöhtem Maße nachweisbar sind.



## ACKNOWLEDGEMENTS

---

I would like to thank professor Xin Lu for hosting me in her lab at the Oxford Ludwig Institute. She has guided me through the ups and downs of my project with kindness and patience, and her continuous support has helped me to grow as a researcher.

Furthermore, I would like to express my thanks to the Lu lab and all the people at the Ludwig Institute for the stimulating discussions, laughs and for making me feel welcome from my first day on.

I am also thankful for the great support I have received from Fabian Becker and my mother, Krystyna Pinner. Without them my stay in Oxford would not have been possible.

Finally, I would like to thank the European Union for funding my stay at the University of Oxford with an Erasmus+ grant.



## CONTENTS

---

1	INTRODUCTION	1
1.1	The p53 protein family . . . . .	1
1.2	The role of p63 in health and disease . . . . .	2
1.3	The role of p73 in health and disease . . . . .	4
1.4	Human Papillomavirus and cancer . . . . .	5
1.5	Aim of the thesis . . . . .	7
2	MATERIALS AND METHODS	9
2.1	Chemicals . . . . .	9
2.2	Materials and devices . . . . .	10
2.2.1	Water, buffers and solutions . . . . .	10
2.2.2	SDS-polyacrylamide gels . . . . .	10
2.2.3	Genes, plasmids and IVTT . . . . .	10
2.2.4	Antibodies . . . . .	12
2.2.5	Western blot, film development and image analysis . . . . .	13
2.3	Experimental procedures . . . . .	14
2.3.1	In vitro transcription and translation (IVTT) . . . . .	14
2.3.2	SDS-PAGE and Western Blot . . . . .	15
2.3.3	Optimisation of IVTT reaction conditions . . . . .	16
2.3.4	Degradation of p53 family members . . . . .	17
2.3.5	Degradation of p53 in presence of p63 or p73 . . . . .	18
2.3.6	Time-resolved degradation of p53 and $\Delta$ Np63 $\alpha$ . . . . .	19
2.3.7	Degradation assay with varying concentrations of 18E6, NaCl or DTT . . . . .	19
2.3.8	Degradation assay with heat shocked p53 . . . . .	20
2.3.9	IVTT of HIF1 $\alpha$ and 18E6 in presence of NOG . . . . .	21
2.3.10	Degradation of p53 in presence of NOG . . . . .	22
2.3.11	IVTT of 18E6 at different pH values . . . . .	22
3	RESULTS	25
3.1	Plasmid and ion concentrations influence yield in IVTT . . . . .	25
3.2	p63 and p73 are targeted for degradation by HPV-16 E6 . . . . .	26
3.3	$\Delta$ Np63 $\alpha$ can slow down the degradation of p53 . . . . .	30
3.4	Heat shocked p53 cannot be degraded by E6 . . . . .	32
3.5	N-Oxalylglycine influences protein yields in IVTT . . . . .	33
4	DISCUSSION	37
4.1	Plasmid and ion concentrations influence yield in IVTT . . . . .	37
4.2	p63 and p73 are targeted for degradation by HPV-16 E6 . . . . .	38
4.3	$\Delta$ Np63 $\alpha$ can slow down the degradation of p53 . . . . .	40
4.4	Heat shocked p53 cannot be degraded by E6 . . . . .	41
4.5	N-Oxalylglycine influences protein yields in IVTT . . . . .	41
5	SUMMARY AND CONCLUSION	45
	BIBLIOGRAPHY	47

## ACRONYMS

---

2OG	2-Oxoglutarate
GC	Gas Chromatography
HIF	Hypoxia-Inducible Factor
HPV	Human Papillomavirus
HRP	Horseraddish Peroxidase
IVTT	In Vitro Transcription and Translation
JMJD	Jumonji Domain ( <i>Oxygenase</i> )
LB	Lysogeny Broth
NF	Nuclease-Free
PA	Polyacrylamide
PAGE	Polyacrylamide Gel Electrophoresis
PHD	Prolyl Hydroxylase Domain ( <i>Oxygenase</i> )
RRL	Rabbit Reticulocyte Lysate
RT	Room Temperature
TAD	Transactivation Domain
TBST	TRIS-Buffered Saline with Tween20
VC	Vector Control
UP	Ultra Pure

For acronyms of chemicals compounds not listed here, please refer to table [1](#) on page [9](#).

## INTRODUCTION

---

### 1.1 THE P53 PROTEIN FAMILY

Tumour protein 53 (gene: *TP53*; protein: p53;) is an important transcription factor involved in the regulation of cell cycle and apoptosis<sup>1</sup>. Disruption of the p53 signalling pathways either through mutation of *TP53* itself or inactivating mutations of critical downstream targets results in a tumour prone phenotype<sup>1</sup>. This observation is especially evident in patients with Li-Fraumeni syndrome (an autosomal dominant disorder caused by germ-line mutations in the *TP53* gene) who have a very high chance of developing various forms of cancers throughout their lifetime<sup>2</sup>. *TP53* is the most commonly mutated gene in human cancers and its gene product p53 plays an important role in tumour suppression<sup>1</sup>.

p53 is kept at low basal levels through interactions with E3 ubiquitin ligases (most notably MDM2) which ubiquitinate and thereby mark it for proteasomal degradation<sup>1</sup>. However, in response to cellular stresses such as DNA damage or hyperproliferation p53 is stabilised and rapidly accumulated by uncoupling it from MDM2<sup>1</sup>. Depending on the type and severity of the stress, an adequate response in the form of DNA damage repair, senescence or apoptosis is triggered by post-translationally modified p53<sup>1</sup>. However, in most human cancers this signalling network is impaired. While early precursor lesions commonly show constitutive activation of DNA damage signalling pathways, more advanced cancers tend to gradually lose the expression of key actors in the damage response, including p53<sup>1</sup>. This process ultimately increases the genetic instability of the cell and thereby accelerates cancer progression<sup>1</sup>.

In nearly every second human cancer, the tumour suppressive function of p53 is lost through direct mutations of *TP53*<sup>3</sup>. In the remaining cases p53 function is commonly lost indirectly either through the inactivation of key factors required for the stabilisation of p53, or through the overexpression of MDM2 as a negative regulator of p53<sup>3</sup>. In either case, the affected cells lose important defence mechanisms which drives carcinogenesis.

In the late 1990s two proteins were discovered which showed homology to p53 in sequence and structure<sup>4-7</sup>. Along with p53, these proteins, termed p63<sup>5</sup> and p73<sup>7</sup>, form the p53 protein family. Phylogenetic analyses have revealed that p63 was the founding member of the family, followed by p73 and lastly p53<sup>8</sup>. The protein structure consists of an N-terminal transactivation domain (TAD) serving as binding site for positive and negative regulators of gene expression, followed by a proline-rich sequence recognition domain (PRD), a centrally located DNA-binding domain (DBD) which recognises response elements of target genes, and a C-terminal oligomerisation

domain (OD)<sup>8</sup>. Unlike p53, full-length p63 and p73 further carry a sterile alpha motif domain (SAMM) involved in protein-protein interactions, as well as a transactivation inhibitory domain (TID) which binds TAD to prevent constitutive transcriptional activity<sup>8</sup>. A particularity of the p53 gene family is the presence of cryptic internal promoters that give rise to full-length (carrying a TAD) TA or truncated (having in part lost the TAD)  $\Delta$ N protein isoforms<sup>8</sup>. Furthermore, several splice sites give rise to a number of distinct C-terminal splice variants, each of which has been assigned a Greek letter (e.g. TAp63 $\alpha$  and  $\Delta$ Np63 $\beta$ )<sup>8</sup>. Currently, 12 different isoforms of p53 are known with four distinct N-termini (one of which is due to alternative initiation of translation) and three C-terminal splice variants (p53 (full-length),  $\Delta$ N44p53,  $\Delta$ N133p53,  $\Delta$ N160p53; - $\alpha$ , - $\beta$ , - $\gamma$ );<sup>8-10</sup>. The p63 gene is currently known to produce at least 10 isoforms from two promoters and five C-terminal variants (TA/ $\Delta$ Np63 $\alpha$ - $\epsilon$ );<sup>8</sup>. In addition, a third N-terminal variant called GTAp63 that is almost exclusive to the male germ-line of humans and great apes was discovered in 2011<sup>11</sup>. The p73 gene can produce at least 14 isoforms from two promoters and seven C-terminal splice variants (TA/ $\Delta$ Np73 $\alpha$ - $\eta$ );<sup>8</sup>. p53, TAp63 and TAp73 form tetramers for transactivation of target genes and while all of them can form homotetramers, TAp63 and TAp73 can also form heterotetramers together<sup>12</sup>. Moreover, p53, TAp63 and TAp73 bind to similar consensus sequences owing to their structural and sequence homology<sup>12</sup>. Despite having partially overlapping functions, each member of the protein family also carries out specialised functions among which some may be limited to specific isoforms and their unique properties<sup>8</sup>.

## 1.2 THE ROLE OF P63 IN HEALTH AND DISEASE

TAp63 and  $\Delta$ Np63 are widely expressed in adult human tissues, but not necessarily at the same time<sup>13</sup>. Paraffin sections of human tissues probed with antibodies against p63 have shown prominent nuclear staining of basal epithelial cells, with a diminution of staining in more terminally differentiated cell layers and no detectable staining in the most superficial cell layers<sup>5,14</sup>. Several studies have revealed that  $\Delta$ Np63 is the predominant isoform within these layers whereas TAp63 is barely detectable<sup>13,15,16</sup>. However, TAp63 is highly expressed in oocytes<sup>17</sup> and testicular tissue<sup>11</sup> as well as being the first isoform to be expressed before the initiation of epithelial stratification during embryonic development<sup>18</sup>. p63 has not been found to be expressed in mesenchymal cells or muscle cells<sup>14</sup>, but it does play a role in neuronal development<sup>19</sup>.

The role of p63 in mammalian development was studied in *TP63*<sup>-/-</sup> mice. These mice displayed several developmental defects, including no epidermis, abnormal squamous epithelia and a lack of epithelial appendages such as mammary glands, hair follicles, and teeth<sup>17</sup>. Furthermore, they had truncated limbs, showed abnormal craniofacial development and died soon after birth<sup>17</sup>. Similar observations have been made in humans, where mutations in one of the two p63 genes are associated with abnormalities of ectodermal

structures such as hair, teeth, nails, sweat glands, craniofacial structures, and digits<sup>17</sup>. Murine  $\Delta Np63$  plays an important role in the terminal differentiation of epidermal cells and possibly also in the proliferation of stem cells<sup>12</sup>. This data emphasises the role of p63 in a regulatory network controlling epithelial and limb development<sup>17</sup>.

Transactivation studies conducted with numerous isoforms of p63 have revealed that p63 target genes are mainly activated by TAp63 $\alpha$  and - $\beta$ , while the shorter TAp63 $\gamma$  showed no such activity<sup>20</sup>. In contrast, even though all three of these isoforms can also bind to promoters carrying a p53 binding site, TAp63 $\gamma$  exhibits the strongest transcriptional activation of these genes comparable to transactivation by p53 itself<sup>5,21</sup>. Owing to its structural resemblance to p53, TAp63 $\gamma$  is also the most transcriptionally active isoform of p63 to induce apoptosis<sup>12</sup>. Among the currently known functions of TAp63 are the induction of cell-cycle arrest, senescence, DNA repair, and apoptosis - all of which can be triggered independently of p53<sup>5,6,17</sup>.

Despite being rarely mutated or deleted in cancer, the *TP63* gene is often deregulated or overexpressed<sup>17</sup>. Tumours that are associated with poor prognosis commonly overexpress C-terminal variants of  $\Delta Np63$ <sup>17</sup>. In similarity to p53, genotoxic stress such as chemotherapy triggers a rapid accumulation of TAp63<sup>12,17</sup>. At the same time, genotoxic stress destabilises  $\Delta Np63$  and in this way promotes its proteasomal degradation<sup>12</sup>. This mechanism leads to a relative shift of the TA/ $\Delta N$  ratio towards TAp63, whose functions include the induction of cell-cycle arrest, senescence, DNA repair, and apoptosis - all of which can be triggered independently of p53<sup>17</sup>. TAp63 also prevents invasiveness and acts as an important suppressor of metastasis by controlling the expression of a crucial set of metastasis-inhibitor genes<sup>12,17</sup>. This first became evident in mice double heterozygous for p53 and p63. Among those which have developed tumours, 90% progressed to metastatic disease which stands in contrast to mere 5% in mice heterozygous for just p53<sup>12</sup>. Because of its ability to transactivate genes involved in apoptosis, senescence and maintaining stem cells in quiescence, TAp63 is widely seen as a tumour suppressor<sup>12</sup>. It is highly expressed in oocytes<sup>17</sup> as well as in spermatogenic progenitor cells (in the form GTAp63<sup>11</sup>) and has therefore been dubbed the 'guardian of human reproduction' by some researchers<sup>22</sup>.

The function of  $\Delta Np63$  is more complex than that of TAp63. The various isoforms of  $\Delta Np63$  have the ability to interfere with the tumour suppressive functions of p53, TAp63 and TAp73 by competing with them for DNA consensus sites in a dose-dependent manner<sup>12</sup>. However, despite lacking a transactivation domain as found in TAp63,  $\Delta Np63$  possesses a unique N-terminal proline-rich transactivation domain allowing it to activate gene transcription independently of p53 or TAp63<sup>12,23,24</sup>. The transcriptional activity of  $\Delta N$  isoforms of p63 is often low, but exceptions exist where transactivation can be comparable to or a lot stronger than transactivation by their TA counterparts<sup>5,21,23</sup>.

$\Delta Np63$  combines the oncogenic feature of interfering with its tumour suppressive sister proteins with the tumour suppressive feature of being a po-

tent transcriptional activator of genes involved in DNA repair<sup>12</sup>. Moreover, some human tumours overexpress  $\Delta$ Np63 as is common for oncogenes, while others stop expressing it as is common for tumour suppressors<sup>12</sup>. A number of studies has found a connection between gradual loss of p63 expression and tumour progression, where low or undetectable levels of p63 are associated with higher aggressiveness of tumours, dedifferentiation, invasiveness and also reduced survival<sup>12,25-27</sup>. It is thought that  $\Delta$ Np63 is involved in the regulation of development, morphogenesis, proliferation, tissue regeneration, cell adhesion, death, and signalling pathways<sup>17</sup>.

### 1.3 THE ROLE OF P73 IN HEALTH AND DISEASE

Expression profiling of TA- and  $\Delta$ Np73 $\alpha$  in humans has revealed tissue specific expression of these isoforms at low or moderate levels, which stands in stark contrast to the ubiquitous expression of p53<sup>28,29</sup>. While strong to moderate expression of p73 was detected in several organs, it was virtually absent in others<sup>28</sup>. In similarity to p63, p73 $\alpha$  is strongly expressed in basal cells of various epithelia with a gradual decrease of expression levels as the cells differentiate<sup>28</sup>. No expression of p73 $\alpha$  has been detected in mesenchymal elements, lymphocytes or organs such as liver, spleen, thyroid and placenta<sup>28</sup>.

*TP73*<sup>-/-</sup> mouse models have been created to study the physiological roles of p73 in life and development. These mice display developmental defects and die early due to recurring inflammation and infections<sup>30</sup>. Of particular interest is the role of p73 in the central nervous system as the knockout mice showed many neurological defects<sup>30</sup>. Heterozygous *TP73*<sup>+/-</sup> mice, when aged, develop an Alzheimer like phenotype<sup>30</sup>.

A softer approach where only TAp73 or  $\Delta$ Np73 was knocked out gave a more detailed image of the involvement of these two groups of isoforms that differed from the complete KO phenotype. Mice lacking TAp73 showed malformations of the hippocampal dentate gyrus, but none of the other neurological defects observed in the complete knockout models<sup>30</sup>. Similarly,  $\Delta$ Np73 knockout mice displayed several less severe neurological defects than those in complete KO mice<sup>30</sup>. The experiments conducted in mice have revealed the importance of p73 in the development and maintenance of the central nervous system. While  $\Delta$ Np73 is required for neuronal survival, TAp73 is required for maintenance and differentiation of neuronal stem cells<sup>30</sup>.

Among the non-neurological consequences of TAp73 knockout are chromosomal instability and the formation of spontaneous tumours, suggesting a tumour suppressive role for TAp73<sup>30</sup>. Treatment of cells with DNA damaging agents can lead to a 2- to 3-fold increase in TAp73 mRNA and indicates an involvement of TAp73 in the DNA damage response<sup>31</sup>. In contrast,  $\Delta$ Np73<sup>-/-</sup> mice do not display a tumour prone phenotype<sup>30</sup>. The properties of the TA and  $\Delta$ N isoforms are similar to those of p63. TAp73 is a regulator of cell cycle arrest and apoptosis while  $\Delta$ Np73 competes with p53 and TAp73 for DNA binding sites or interferes with TAp73 function by forming

heteroduplexes<sup>31–33</sup>.  $\Delta Np73\beta$  has been found to be able to induce cell cycle arrest and apoptosis<sup>34</sup>, but it has also been described as a potent inhibitor of TAp73 $\beta$  induced apoptosis<sup>32</sup>. In E1A mouse embryo fibroblasts, a deficiency of both, p63 and p73, at the same time confers resistance to apoptosis to a similar extent as a deficiency of p53<sup>35</sup>.

Despite being unable to associate with wild type p53<sup>31</sup>, p73 can bind certain mutant forms of p53 which functionally inactivates it<sup>36</sup>. A polymorphism of p53 at codon 72 encoding either arginine or proline (72R and 72P, respectively) can influence the binding of mutant p53 to p73<sup>31</sup>. In patients carrying both alleles, p53-72R is especially prone to mutations suggesting a selective advantage of the mutated 72R form in cancer cells<sup>31</sup>. Interestingly, p53-72R was also shown to bind p73 with a greater affinity and consequently inhibit its transactivating activity more efficiently<sup>31</sup>. In this way, binding of p73 by certain mutants of p53 can inhibit p73-dependent apoptosis, with p53-72R mutants being especially effective<sup>31</sup>.

In cancer, p73 is rarely mutated but commonly deregulated<sup>31</sup>. Some cancers like neuroblastomas overexpress p73 isoforms, whereas other malignancies like pancreatic cancers cease to express p73 which predicts worst prognosis<sup>31</sup>. An analysis of healthy and malignant breast tissue has revealed a difference in the p73 isoform expression pattern<sup>31</sup>. Whereas p73 $\alpha$  and p73 $\beta$  are the predominant isoforms in healthy breast tissue, there is a shift towards other isoforms in cancerous tissue<sup>31</sup>. There is increasing evidence that the impact of p73 on tumour progression depends more on the ratio of TA to  $\Delta N$  isoforms rather than the absolute amount of proteins present<sup>31</sup>. Given that  $\Delta Np73$  has a longer half-life than the TA isoforms, overexpression of both isoforms may be biased towards  $\Delta Np63$  as reports have shown<sup>31</sup>. Overexpression of  $\Delta Np73$  without a concomitant increase in TAp73 is associated with poor prognosis and reduced survival<sup>31</sup>. As is the case for p63, chemotherapeutic agents induce the expression of the TA form of p73<sup>32</sup>. TAp73 $\beta$  acts synergistically with the chemotherapeutic drug bleomycin by cooperating at different levels of apoptosis signalling<sup>32</sup>. However, chemotherapeutic agents also induce the expression of  $\Delta Np73$ , which exhibits antipoptotic functions<sup>32</sup>. As a result, the ratio of the two isoforms TAp73/ $\Delta Np73$  is an important determinant of response to chemotherapy<sup>32</sup>.

#### 1.4 HUMAN PAPILLOMAVIRUS AND CANCER

Nearly every case of cervical cancer can be traced back to an infection with an oncogenic type of human papillomaviruses (HPV), immediately suggesting a connection between oncogenesis and virus infection<sup>37</sup>. It has been shown that the risk of developing cervical cancer after infection with oncogenic HPVs is greater than the risk of developing lung cancer from smoking or liver cancer from Hepatitis B virus infection<sup>38</sup>. There are over 150 genotypes of HPV currently known and only a fraction of them ('high-risk' types) are associated with oncogenesis<sup>38</sup>. Among the many types of HPV, the most

prominent high-risk genotypes are HPV16 and HPV18 which are responsible for 60-80% of all cervical cancers<sup>38</sup>.

HPVs are small nonenveloped viruses carrying a circular double-stranded DNA genome approximately 8 kb in size and encoding eight genes<sup>37,39</sup>. The genes of the virus are divided into early (E) and late (L) phase genes and ordered according to their size, where the largest open reading frame has been given the smallest number (1) and vice versa<sup>39</sup>. HPV is known to infect the basal layer of epithelia where the viral DNA is maintained as an extrachromosomal element at a low copy number in the nucleus of the host cell<sup>39,40</sup>. When the infected host cell divides, the viral DNA is distributed between both daughter cells<sup>40</sup>. Following mitosis, one of the daughter cells then undergoes a process of differentiation as it migrates to the upper layers of the epithelium, whereas the other daughter cell remains in the basal layer where it serves as a virus reservoir<sup>40</sup>. In the upper layer of the epithelium, expression of late genes is induced for capsid production and virion assembly<sup>41</sup>. In normal epithelia, cells undergoing differentiation would exit the cell cycle in the process<sup>40</sup>. However, as HPV depends on cellular enzymes for replication of its own genome, cell cycle exit is suppressed in high-risk type HPV infected cells through two viral proteins called E6 and E7<sup>40</sup>. E6 of high-risk HPVs can bind to p53 and promote its ubiquitination and subsequent degradation by recruiting the cellular E3 ubiquitin ligase E6AP<sup>40</sup>. In contrast, low-risk HPV E6 proteins are unable to associate with p53 or do not promote its degradation<sup>40</sup>. In absence of high-risk type E6, E6AP hardly binds to p53 at all which therefore remains unaffected<sup>40,42</sup>. However, viruses of the low-risk type can still block cell cycle exit<sup>40</sup>. E7 proteins of both, high-risk and low-risk HPVs, have the ability to bind to the tumour suppressor protein Rb<sup>40</sup> which is required for cell cycle progression from G1 to S phase<sup>43</sup>. Nevertheless, E7 of high-risk HPV types bind Rb much more efficiently than E7 of low-risk HPVs<sup>37</sup>. Because of the ability of E6 and E7 to interfere with cellular tumour suppressor proteins, they are able to immortalise human cells<sup>44</sup>.

A viral protein that is commonly inactivated in cervical cancer is E2. E2 tethers the viral genome, which is initially kept at less than 50 extrachromosomal, circular units (episomes), to the host chromatin and also functions a gene transcription factor<sup>41,45,46</sup>. One of its most important functions in the carcinogenesis of cervical carcinoma is its ability to repress E6 and E7 transcription by binding to two sites on the viral genome close to the E6/E7 promoter<sup>46</sup>. However, in cervical carcinoma, the viral genome is often integrated into the host cell genome in such a way that E2 is inactivated<sup>45</sup>. In cancer cells where no integration of viral DNA occurs, mutations of E2 or other repressors can instead be detected<sup>45</sup>. Consequently, reintroduction of E2 into cervical cancer cell lines induces cell cycle arrest, senescence or apoptosis<sup>46</sup>. The loss of functional E2 leads to uncontrolled expression of E6 and E7, which, due to their oncogenic properties such as degrading p53, increase genetic instability and promote carcinogenesis<sup>46</sup>.

## 1.5 AIM OF THE THESIS

HPV infection is the cause of virtually every case of cervical cancer<sup>38</sup>. Given the importance of p53 in tumour suppression and the growing understanding of the roles of p63 and p73 in tumour suppression and cancer, the question arose if p63 and p73 were also targeted by E6 for degradation. Studies conducted by Ben Khalifa et al have indeed shown that TA- and  $\Delta$ Np63 $\beta$  are degraded by HPV18-E6 in HeLa cells, though via a pathway that is independent of E6AP<sup>20</sup>. To our knowledge, other isoforms of p63 have previously not been tested. Similar experiments have also been conducted with p73, but with negative results claiming that E6 cannot promote the degradation of p73<sup>47-49</sup>. This thesis aims to explore the potential of E6 to degrade the various isoforms of p63 and p73 in vitro. Positive results may provide further insights into the mechanisms by which HPV drives carcinogenesis. The basic experimental setup for in vitro degradation assays is based on the work of Scheffner et al<sup>50</sup>. In the process, the experimental conditions for in vitro transcription and translation are optimised. Furthermore, the mechanism by which p53 is degraded by E6 is studied by inhibiting 2-oxoglutarate dependent oxygenases to determine if hydroxylation of p53 is required for the binding of E6.



## MATERIALS AND METHODS

## 2.1 CHEMICALS

**Table 1** List of used chemicals

Name (acc. suppl.)	Abbr.	Suppl.	Mw	Notes
2-Propanol		Sigma-Aldrich	60.10	≥ 99.5%, meets anal. spec.
Acrylamide, Bis-acrylamide		Severn Biotech		30% Stock solution (w/v), 37.5:1 Bisacrylamide
Ammonium persulfate	APS	Fisher scientific	228.20	
Bromophenol Blue		Sigma-Aldrich	669.98	
Citric Acid anhydrous		Fisher scientific	192.13	general purpose grade
Dimethyl sulfoxide	DMSO	Sigma-Aldrich	78.13	≥ 99.9%, A.C.S. spectrophotometric grade
Dithiothreitol	DTT	Fluorochem	154.24	
Dried skimmed Milk		Premier Foods		<1% fat
Glycerol		Sigma-Aldrich	92.09	≥ 99.0% (GC)
Glycine		Fisher Chemical	75.07	anal. reagent grade
HEPES		Sigma-Aldrich	238.30	≥ 99.5% (titration)
Hydrochloric acid	HCl	Fisher scientific	36.46	~ 37%, anal. reagent grade
Methanol	MeOH	Sigma-Aldrich	32.04	≥ 99.8% (GC), p.a.
MG132		Merck	475.63	≥ 98%
NNN'N'-Tetramethylethylene diamine	TEMED	Fischer scientific	116.21	
N-Oxalylglycine	NOG	self synthesised	147.09	kindly provided by Prof. Chris Schofield
Ponceau-S solution		Sigma-Aldrich	750.57	0.1% (w/v) in 5% acetic acid, suitable f. electroph.
Sodium acetate	NaAc	BDH	82.03	anhydrous
Sodium Azide, 1%	NaN <sub>3</sub>	Severn Biotech Ltd.		1% solution
Sodium Chloride	NaCl	Fisher scientific	58.44	anal. reagent grade
Sodium Citrate Dihydrate		Fisher scientific	294.09	small, colourless granules
Sodium Dodecyl Sulphate	SDS	Fisher scientific	288.5	micropellets
SDS solution	SDS	Severn Biotech Ltd.		10% sol., Mol. Biol. Grade
Sodium Hydroxide	NaOH	Fisher scientific	40	white pellets
TRIS-Base	TRIS	Fisher scientific	121.14	white crystals
Tween <sup>®</sup> 20		Fisher scientific	1227.54	
Urea		Sigma-Aldrich	60.06	powder

## 2.2 MATERIALS AND DEVICES

### 2.2.1 *Water, buffers and solutions*

Two sources of purified water were used to dissolve chemicals and for use in experiments: ELGA PURELAB Option (resistivity: 15.0 M $\Omega$ .cm) and ELGA PURELAB Ultra (resistivity: 18.2 M $\Omega$ .cm). Unless stated otherwise, the term UP-H<sub>2</sub>O refers to the ELGA PURELAB Ultra system with a resistivity of 18.2 M $\Omega$ .cm in this thesis, while the ELGA PURELAB Option system was used in cases where water purity was not critical (e.g. large volumes of buffers). Table 2 below lists buffers and solutions that were used in the experiments.

### 2.2.2 *SDS-polyacrylamide gels*

Gels intended for SDS-PAGE were prepared as stated in table 3 below<sup>51</sup>. The gels were cast using the Mini-PROTEAN<sup>®</sup> Tetra-Handcast system (Bio-Rad). After pouring the resolution gel, the gel was topped up carefully with 1 ml of 2-propanol and left standing for at least 45 mins, after which the 2-propanol was removed and the gel was rinsed with deionised H<sub>2</sub>O. The stacking gel was then poured on top of the polymerised resolution gel and a comb to form a 10 or 15 lane gel was inserted until the gel solidified.

### 2.2.3 *Genes, plasmids and IVTT*

All genes listed in table 4 were cloned into pcDNA3 plasmid vectors. The plasmids were multiplied in *Escherichia coli* chemically competent cells (Subcloning Efficiency<sup>™</sup> DH5 $\alpha$ <sup>™</sup>, Invitrogen) according to the manufacturer's instructions. Transformed bacteria were selected on LB-medium agar plates (+ampicillin) overnight at 37°C and enriched in LB-medium broth containing ampicillin overnight at 37°C. Plasmids were harvested using the QIAprep<sup>®</sup> Spin Miniprep Kit (QUIAGEN) following the manufacturer's protocol. Plasmids were eluted using the elution buffer (10 mM TRIS-Cl, pH 8.5) provided in the kit. The plasmid concentrations were estimated by nanodropping (ND-1000 spectrophotometer NanoDrop<sup>®</sup>, Thermo scientific). The genes were transcribed and translated in vitro using the TNT<sup>®</sup> T7 Quick coupled Transcription/Translation System (Promega, Ref: L1170). If not stated otherwise, this system was used for the synthesis of proteins from plasmids. All required components like RRL-MasterMix, 1 mM methionine solution, NF-water and ion solution (500 mM KCl and 12.5 mM MgAc<sub>2</sub>, "PCR-enhancer") were taken from this kit. For one assay, the TNT<sup>®</sup> T7 coupled Reticulocyte System (Promega, Ref: L4610) was used. The components of this kit and RNase A (Promega) were mixed according to the manufacturer's instructions.

**Table 2** Buffers and solutions used for all experiments

<b>Buffer / Solution</b>	<b>Composition</b>
resolution gel buffer	1.5 M TRIS adjusted to pH 8.8 with HCl autoclaved
stacking gel buffer	1 M TRIS adjusted to pH 6.8 with HCl and NaOH autoclaved
assay buffer (3x)	75 mM TRIS 300 mM NaCl adjusted to pH 7.4 with HCl autoclaved
TBST (20x)	400 mM TRIS 2.74 M NaCl adjusted to pH 7.4 with HCl autoclaved 20 ml Tween20 per 1 l 20x buffer
sample buffer (6x)	520 mM SDS < 2 mM Bromophenol blue 60% (v/v) Glycerol 7.5% (v/v) 1 M TRIS buffer (pH 6.8) 32.5% (v/v) UP-H <sub>2</sub> O
running buffer (10x)	1.92 M Glycine 0.25 M TRIS 35 mM SDS
transfer buffer (10x)	1.93 M Glycine 0.24 M TRIS
DTT solution (1 M)	0.01 M NaAc pH adjusted to 5.2 with HCl 1 M DTT
blocking buffer	5 g dried skimmed milk 5 ml TBST (20x) 95 ml purified H <sub>2</sub> O

**Table 3** Gel recipes for SDS-PAGE<sup>51</sup>

<b>Gel percentage</b>	<b>Components [10 ml]</b>
8%	4.6 ml UP-H <sub>2</sub> O 2.7 ml 30% acrylamide mix 2.5 ml 1.5 M TRIS (pH 8.8) 0.1 ml 10% SDS 0.1 ml 10% APS 0.006 ml TEMED
12%	3.3 ml UP-H <sub>2</sub> O 4.0 ml 30% acrylamide mix 2.5 ml 1.5 M TRIS (pH 8.8) 0.1 ml 10% SDS 0.1 ml 10% APS 0.004 ml TEMED
15%	2.3 ml UP-H <sub>2</sub> O 5.0 ml 30% acrylamide mix 2.5 ml 1.5 M TRIS (pH 8.8) 0.1 ml 10% SDS 0.1 ml 10% APS 0.004 ml TEMED
stacking gel	6.8 ml UP-H <sub>2</sub> O 1.7 ml 30% acrylamide mix 1.25 ml 1.0 M TRIS (pH 6.8) 0.1 ml 10% SDS 0.1 ml 10% APS 0.01 ml TEMED

#### 2.2.4 Antibodies

Table 5 below lists the antibodies that were used for western blotting purposes. All antibodies were diluted in blocking buffer with added NaN<sub>3</sub> at a final concentration of 0.01%. The species targeted by the antibody is stated in brackets in the target column, where (h) stands for human, (m) for mouse and (r) for rabbit.

**Table 4** Constructs used for in vitro transcription & translation

<b>Gene</b>	<b>Tag</b>	<b>Vector</b>	<b>Species</b>
p53 (Pro72)	-	pcDNA3	human
TAp63 $\alpha$	HA	pcDNA3	human
TAp63 $\gamma$	myc	pcDNA3	mouse
$\Delta$ Np63 $\alpha$	HA	pcDNA3	human
$\Delta$ Np63 $\beta$	HA	pcDNA3	human
$\Delta$ Np63 $\gamma$	myc	pcDNA3	mouse
TAp73 $\alpha$	HA	pcDNA3	human
TAp73 $\beta$	V5	pcDNA3	human
TAp73 $\gamma$	HA	pcDNA3	human
TAp73 $\delta$	HA	pcDNA3	human
$\Delta$ Np73 $\alpha$	HA	pcDNA3	human
$\Delta$ Np73 $\beta$	V5	pcDNA3	human
HPV-5 E6	HA	pcDNA3	HPV
HPV-8 E6	HA	pcDNA3	HPV
HPV-16 E6	HA	pcDNA3	HPV
HPV-18 E6	HA	pcDNA3	HPV
HIF1 $\alpha$	-	pcDNA3	human

### 2.2.5 Western blot, film development and image analysis

For western blotting, Amersham Protran nitrocellulose membranes (pore size: 0.45  $\mu$ m) by GE health care were used. Results from western blots were obtained by exposing Fuji medical X-Ray films Super XN (Fujifilm Corporation). Exposed films were developed using a SRX-101A film processor (Konica Minolta). The chemicals used to develop (RG Universal RTU X-Ray Developer) and fix (RG Universal RTU X-Ray Fixer) the films were purchased from Champion imaging Ltd. Band intensities were quantified using the open source computer software 'ImageJ'.

**Table 5** Antibodies used for western blotting. The species targeted by the antibody is shown in brackets in the 'target' column, where (h) stands for human, (m) for mouse and (r) for rabbit.

Target	Clone	Supplier	Dilution	Notes
p53 (h)	DO-1	self-made	1:10000	mouse mAb.
p53 (h)	DO-1	self-made	1:2000	mouse mAb.
p73 (h, m)	EP436Y	Abcam	1:1000	rabbit mAb. Ref: ab40658
HIF1 $\alpha$ (h)	54/HIF-1 $\alpha$	BD Bioscience	1:1000	mouse mAb. Ref: 610959
myc-tag	9E10	self-made	1:1000	mouse mAb.
HA-tag	HA-7	Sigma-Aldrich	1:10000	mouse mAb. Ref: H9658
p53 (h) & HA-tag	DO1 + HA-7	self-made & Sigma-Aldrich	1:13333.3 1:10000	mouse mAbs.
Igs (m)	<i>polyclonal</i>	Dako	1:2000	rabbit Abs. HRP-coupled Ref: P0161
Igs (r)	<i>polyclonal</i>	Dako	1:2000	swine Abs. HRP-coupled Ref: P0217

### 2.3 EXPERIMENTAL PROCEDURES

#### 2.3.1 *In vitro* transcription and translation (IVTT)

Sample proteins were synthesised using the T7 TnT<sup>®</sup> Quick Coupled Transcription/Translation system by Promega. The following protocol is valid for all experiments unless stated otherwise.

*The reaction volume was adjusted according to the quantity of protein needed.*

One volume of IVTT reaction mixture contained 0.8 vol T7 TnT<sup>®</sup> Quick Master Mix ('RRL-MasterMix', contains rabbit reticulocyte lysate (RRL)), 0.1 vol plasmid solution (50 ng/ $\mu$ l), 0.08 vol nuclease-free water (NF-water) and 0.02 vol methionine solution (1 mM). To receive sufficient and detectable amounts of protein, some reactions were supplemented with 0.05 vol of a solution of 500 mM KCl and 12.5 mM MgAc<sub>2</sub> to increase the translation efficiency. In these cases, the amount of NF-water was reduced accordingly to 0.03 vol. The reactions were incubated at 30°C for 1.5 h and instantly used for any following steps.

### 2.3.2 SDS-PAGE and Western Blot

Any protein samples to be separated by SDS-polyacrylamide gel electrophoresis (SDS-PAGE) were undertaken a denaturation step either by boiling or by incubation in urea solution. For heat denaturation, the samples were mixed with 6 x protein sample buffer and 1 M DTT solution to a final concentration of 1-2.5 x sample buffer and 100 mM DTT. The samples were boiled at 97°C for 5 min unless stated otherwise and spun down. For denaturation in urea, the samples were mixed with freshly prepared 10 M urea solution and incubated at 25°C for 20 min. Then, the samples were mixed with 6 x protein sample buffer and 1 M DTT solution to a final concentration of 1.5-2.5 x sample buffer and 100 mM DTT and incubated for 10 min at 25°C after which the samples ready to be loaded onto polyacrylamide gels.

The density of the SDS-polyacrylamide gels ranged from 8% to 15% and was chosen according to the molecular weight of the proteins of interest. The electrode assembly holding the SDS-polyacrylamide gels was placed into a tank and filled up with running buffer. Then the tank was filled up with running buffer itself and aliquots of the sample solutions were carefully loaded onto the SDS-polyacrylamide gels of appropriate density to separate the proteins of interest from one another. The SDS-PAGE was run at constant voltage, though manual adjustments were made throughout the electrophoresis where necessary. Once the SDS-PAGE had finished, the polyacrylamide gels were removed from their glass cassettes and assembled into a transfer sandwich along with a nitrocellulose membrane (0.45  $\mu\text{m}$ ). All components of the sandwich (sponges, filter papers, membranes and gels) were immersed in transfer buffer prior to use, and the assembled sandwiches were put into a transfer tank filled with transfer buffer. The proteins were transferred overnight at 30 V and 4°C.

Success of protein transfer was confirmed by immersing the membranes in Ponceau S solution followed by removal of the dye using cold tap water. The membranes were blocked in blocking buffer for 1 h at RT under gentle agitation and then probed for the proteins of interest using suitable primary antibody solutions (primary antibody in blocking buffer) at RT for 1 h under gentle agitation unless stated otherwise. Excess antibodies were removed by rinsing the membranes with cold tap water and three incubation steps in TBST (10 min, RT). The membranes were then incubated in secondary antibody solution (HRP-coupled anti-mouse antibody in blocking buffer) at RT for 1 h under gentle agitation, rinsed under cold tap water followed by three incubation steps in TBST (10 min, RT) to remove unbound antibodies. For detection of proteins, ECL reagent (GE healthcare) was applied onto the membranes according to the manufacturer's instructions. The membranes were then transferred into a film cassette for exposure of an X-ray film. Finally, the X-ray film was inserted into a film developer to reveal protein bands.

### 2.3.3 Optimisation of IVTT reaction conditions

The in vitro synthesis of proteins from plasmid DNA is a simple and quick method to obtain sufficient amounts of protein for further experiments. However, the translation efficiency and thus the amount of protein produced depends a lot on the reaction conditions such as plasmid concentration or ion strength, and it is also affected by the plasmid itself. The reaction conditions must therefore be optimised for each plasmid individually.

#### 2.3.3.1 Variation of plasmid concentration, broad range (5-20 ng/ $\mu$ l)

Several plasmids containing genes of the p53-family (p53,  $\Delta$ Np63 $\alpha$ , TAp63 $\alpha$ , TAp73 $\alpha$ ) and E6 proteins from four different HPV strains (HPV-5, HPV-8, HPV-16 and HPV-18) were tested for the optimal concentration to be used in IVTT reactions. The TnT<sup>®</sup> Coupled Reticulocyte Lysate System (Promega) was used for this experiment and the RRL-MasterMix was prepared according to the protocol provided by the manufacturer. To 6  $\mu$ l RRL-MasterMix, 1-4  $\mu$ l of the plasmid solutions (50 ng/ $\mu$ l) was added to achieve plasmid concentrations of 5, 10, 15 or 20 ng/ $\mu$ l and the reaction volume was filled up to 10  $\mu$ l with NF-water. The reactions were incubated at 30°C for 1.5 h. In separate tubes, 2  $\mu$ l of the translation products were diluted in assay buffer containing approximately 100 mM DTT and 1 x sample buffer. The sample solutions were heated up to 70°C for 10 min, electrophoresed on SDS-PA gels and transferred onto nitrocellulose membranes at 80V for 2.5 h. The membranes were then blocked for 1h in blocking buffer under gentle agitation followed by incubation in DO1 (p53, 1:2000 dilution) or anti-HA (all other sample proteins) antibody dilutions in blocking buffer at 4°C overnight. Excess antibodies were removed by three washing steps in followed by incubation of the membranes in secondary antibody dilutions in blocking buffer for 1h at room temperature and three more washing steps in TBST for 10 minutes each. The blots were developed by soaking the membrane surfaces in ECL developing solution followed by exposure of an X-ray film to the blot.

#### 2.3.3.2 Variation of plasmid concentration, broad range (5-20 ng/ $\mu$ l)

$\Delta$ Np63 $\alpha$  was translated with lower plasmid concentrations than recommended by the manufacturer of the IVTT kit. Five translation reactions with plasmid concentrations ranging from 3-7 ng/ $\mu$ l were prepared and incubated at 30°C for 1.5 h. The samples were denatured by diluting 4  $\mu$ l translation product to a final volume of 100  $\mu$ l (containing 100 mM DTT and 1.5x sample buffer in UP-H<sub>2</sub>O) and subsequently boiling them at 97°C for 5 min. Half of the sample volumes was loaded onto a polyacrylamide gel for SDS-PAGE, and the separated proteins were transferred onto a nitrocellulose membrane overnight. The membrane was blocked and probed for  $\Delta$ Np63 $\alpha$  with anti-HA antibody solution (TBST-5% Milk). After three washing steps with TBST (10 min each), the membrane was incubated in HRP-conjugated anti-mouse secondary antibody solution in blocking buffer (1 h, RT) followed by three more washing steps with TBST (10 min each). Protein bands were revealed

by immersing the membrane in ECL reagent and exposing an X-ray film to the blot.

### 2.3.3.3 Variation of ion concentration

Protein  $\Delta\text{Np63}\alpha$  was translated from plasmids at a plasmid concentration of 3 ng/ $\mu\text{l}$  and five different ion concentrations (KCl [M], MgAc<sub>2</sub> [mM]: +0.00, 0.00; +0.01, 0.25; +0.025, 0.625; +0.04, 1.0; +0.05, 1.25;) while using the amounts of RRL-MasterMix and methionine recommended by the manufacturer of the IVTT-kit. The ion strength was varied by addition of different amounts of a KCl and MgAc<sub>2</sub> stock solution provided by the manufacturer to the reactions ("PCR-enhancer", Promega). The reactions were incubated at 30°C for 1.5 h. The samples were denatured by diluting 4  $\mu\text{l}$  translation product to a final volume of 100  $\mu\text{l}$  (containing 100 mM DTT and 1.5x sample buffer in UP-H<sub>2</sub>O) and subsequently boiling them at 97°C for 5 min. Half of the sample volumes was loaded onto a polyacrylamide gel for SDS-PAGE, and the separated proteins were transferred onto a nitrocellulose membrane overnight. The membrane was blocked and probed for  $\Delta\text{Np63}\alpha$  with an anti-HA antibody solution (TBST-5% Milk). After removal of excess antibodies by three washing steps with TBST (10 min each), the membrane was incubated in HRP-conjugated secondary antibody solution in blocking buffer for 1 h at RT. After three more washing steps with TBST (10 min each), protein bands were revealed by immersing the membrane in ECL reagent and exposing an X-ray film to the blot.

*Ion concentrations listed are in addition to any ions already present in the RRL-MasterMix.*

### 2.3.4 Degradation of p53 family members

This protocol is adapted from Scheffner et al. (1990)<sup>50</sup>. Tumour protein p53 as well as the p53 protein family members p63 (isoforms  $\Delta\text{Np63}\alpha$ , - $\beta$ , - $\gamma$  (murine) and TAp63 $\alpha$ , - $\gamma$  (murine)) and p73 (isoforms  $\Delta\text{Np73}\alpha$ , - $\beta$  and TAp73 $\alpha$ , - $\beta$ , - $\gamma$ , - $\delta$ ) were assayed for HPV-E6 protein mediated degradation in vitro. The sample proteins as well as HPV-16 E6 (16E6) were produced from plasmids by IVTT and immediately used for the following steps. Synthesis of all isoforms of p63 as well as TAp73 $\beta$  and - $\gamma$  was boosted by addition of KCl and MgAc<sub>2</sub>. In addition to this, an empty vector control was prepared. For assaying E6 mediated degradation of p53 family members, aliquots of the p53, p63 and p73 reaction products were mixed with 3  $\mu\text{l}$  16E6 and 3  $\mu\text{l}$  3x assay buffer (+10 mM DTT) and filled up with UP-H<sub>2</sub>O to a total volume of 9  $\mu\text{l}$ . For each of the samples, a negative control was prepared composed of the respective p53/p63 or p73 IVTT product aliquot, 2.5  $\mu\text{l}$  RRL-MasterMix (+Met) as a substitution for 16E6, 3  $\mu\text{l}$  3x assay buffer (+10 mM DTT) and enough UP-H<sub>2</sub>O to achieve a total volume of 9  $\mu\text{l}$ . The samples were incubated at 25°C for 3 h or overnight (16.5 h) at 25°C or 4°C. The reactions were stopped by addition of 9  $\mu\text{l}$  Urea (10 M) and subsequent incubation at 25°C for 20 min. Then, a mixture of 7  $\mu\text{l}$  6x sample buffer and 3  $\mu\text{l}$  DTT (1 M) was added and the samples were incubated for 10 min at 25°. The samples were separated by SDS-PAGE (8% SDS-PA gels) followed by transfer from the polyacrylamide gels onto

*Aliquot sizes were determined empirically for each protein with clearly visible bands as a goal.*

*RRL-MasterMix (+Met) makes up 82% of the IVTT reaction mixture. Therefore, 3  $\mu\text{l}$  16E6 IVTT product contains 2.5  $\mu\text{l}$  RRL-MasterMix (+Met)*

nitrocellulose membranes at 4°C overnight. After protein transfer, the membranes were blocked and subsequently probed for the sample proteins with mouse (DO1 + anti-HA-tag; anti-HA-tag; anti-myc;) or rabbit (anti-p73;) antibodies. Excess antibodies were removed by three washing steps with TBST after which the membranes were incubated in the appropriate HRP-coupled secondary antibodies (rabbit anti-mouse or swine anti-rabbit). After three more washing steps with TBST, protein bands were made visible by the use of the ECL system and exposing an X-ray film to the membranes followed by development of the film.

### 2.3.5 Degradation of p53 in presence of p63 or p73

The extent of HPV-E6 protein mediated degradation of p53 in presence of  $\Delta$ Np63 $\alpha$ , TAp63 $\alpha$  or TAp73 $\alpha$  was studied by coincubation of these proteins along with HPV-5, -16 and -18 E6 proteins. The required proteins were produced by IVTT and aliquoted to be used immediately for the following steps. To test if p63 and/or p73 interfere with the degradation of p53, 1  $\mu$ l p53 was mixed with aliquots of either  $\Delta$ Np63 $\alpha$ , TAp63 $\alpha$  or TAp73 $\alpha$ . Each protein combination was prepared four times along with four control samples, which contain p53 only. To three of the four tubes of each protein combination, 5  $\mu$ l E6 was added after an initial incubation step. In order to normalise the expected protein background in all of the samples, RRL-MasterMix (+Met) was added to the tubes until all of them contained the same total amount of RRL-MasterMix (+Met). For this, the chosen aliquot sizes of p53/p63/p73 and the volume of E6 translation product to be added were considered to determine the differences in RRL-MasterMix (+Met) between the samples. Then, 10  $\mu$ l 3x assay buffer (+10 mM DTT) was added to all of the samples and the samples were topped up with UP-H<sub>2</sub>O to 25  $\mu$ l (tubes to which E6 would be added - three per protein combination) or 30  $\mu$ l (tubes to which no E5 would be added - one per protein combination). The samples were incubated for 15 min at 25°C, after which 5E6, 16E6 or 18E6 were added to the respective samples. This was followed by another incubation of the samples for 3 h at 25°C. The reactions were stopped by addition of 17.5  $\mu$ l 6x sample buffer, 13.5  $\mu$ l 3x assay buffer, 7  $\mu$ l DTT (1 M) and 2  $\mu$ l UP-H<sub>2</sub>O followed by boiling the samples at 97°C for 5 min. Half of the sample volume was used for SDS-PAGE (12% SDS-PA gels). Following electrophoresis, the proteins were transferred from the gels onto nitrocellulose membranes at 4°C overnight. Then, the membranes were blocked and subsequently probed for the sample proteins with a mixture of murine DO1 and anti-HA-tag antibodies. Excess antibodies were removed by three washing steps with TBST after which the membranes were incubated with HRP-coupled secondary rabbit anti-mouse antibodies. After three more washing steps with TBST, protein bands were made visible by the use of the ECL system and exposing an X-ray film to the membranes followed by development of the film.

*The aliquot size was determined empirically for each protein with clearly visible bands as a goal.*

*Note: RRL-MasterMix (+Met) makes up 82% of the IVTT product mixture.*

### 2.3.6 Time-resolved degradation of p53 and $\Delta$ Np63 $\alpha$

The sample proteins p53,  $\Delta$ Np63 $\alpha$  and 18E6 were translated in vitro from plasmids. To resolve the influence  $\Delta$ Np63 $\alpha$  may have on HPV-18 E6 mediated degradation of p53, the degradation process was monitored in intervals of 30 min over the course of 3 h. For this, four samples containing either p53 or  $\Delta$ Np63 $\alpha$ , p53 with added 18E6 or p53 with added 18E6 and  $\Delta$ Np63 $\alpha$  were prepared. The volumes added to each tube correspond to eight times the amount necessary for satisfactory results in western blotting, allowing for 7 samples to be drawn (+ 1 dead volume). The volumes of each translation product added were as follows: p53 (8  $\mu$ l),  $\Delta$ Np63 $\alpha$  (32  $\mu$ l) and 18E6 (40  $\mu$ l). To each tube, 80  $\mu$ l of 3 x assay buffer was added, and where necessary RRL-MasterMix (+Met) was added to equalise the total amount of RRL between the tubes. The reactions were topped up to 240  $\mu$ l with UP-H<sub>2</sub>O and incubated at 25°C up to 3 h. Samples were drawn by removing 30  $\mu$ l from the reactions every 30 min, drawing the first sample at the beginning of the incubation period (0 min) and the last sample after 180 min of incubation. Drawn samples were instantly denatured either by addition of a denaturing solution (35  $\mu$ l 6x sample buffer, 23.3  $\mu$ l 3x assay buffer, 10  $\mu$ l 1 M DTT, 1.7  $\mu$ l UP-H<sub>2</sub>O;) and subsequent boiling at 97°C for 5 min, or by addition of 35  $\mu$ l 10 M Urea solution, incubation at 25°C for 20 min, topping up the solution to 100  $\mu$ l by adding 25  $\mu$ l 6x sample buffer and 10  $\mu$ l 1 M DTT solution and another incubation of the sample at 25°C for 10 min. Half of the solution volumes was used to resolve the sample proteins on 12% SDS-polyacrylamide gels. The proteins were transferred from the gels onto nitrocellulose membranes overnight at 4°C. Following protein transfer, the membranes were blocked and subsequently probed for the sample proteins with a mixture of murine DO1 and anti-HA-tag antibodies. Excess antibodies were removed by three washing steps with TBST after which the membranes were incubated with HRP-coupled secondary rabbit anti-mouse antibodies. After three more washing steps with TBST, protein bands were made visible by the use of the ECL system and exposing an X-ray film to the membranes followed by development of the film.

*Protein yield of  $\Delta$ Np63 $\alpha$  was boosted in one of two runs by adding KCl and MgAc<sub>2</sub> as well as reducing added DNA to 0.06 vol.*

*Note: RRL-MasterMix (+Met) makes up 82% of the IVTT product mixture.*

### 2.3.7 Degradation assay with varying concentrations of 18E6, NaCl or DTT

Proteins p53,  $\Delta$ Np63 $\alpha$  and 18E6 were translated in vitro from plasmids. Synthesis of  $\Delta$ Np63 $\alpha$  was boosted by addition of KCl and MgAc<sub>2</sub>. The proteins were used to test the effect that varying concentrations of 18E6, ions or DTT may have on the E6 mediated degradation of p53. Reactions were set up with and without  $\Delta$ Np63 $\alpha$  to test if the presence of this isoform of p63 has any effect on the degradation of p53 at the various conditions tested. Negative controls (containing 0.5  $\mu$ l p53, 4.9  $\mu$ l RRL-MasterMix (+Met), 5  $\mu$ l 3x assay buffer (+10 mM DTT) and 4.6  $\mu$ l UP-H<sub>2</sub>O) were set up in addition to the sample mixtures to be able to estimate the degree of degradation that has occurred. The sample mixtures contained 0.5  $\mu$ l of p53 and either 4  $\mu$ l of

$\Delta$ Np63 $\alpha$  or 3.3  $\mu$ l RRL-MasterMix (+Met) to ensure equal amounts of RRL. Therefore, for each condition tested, two samples were prepared, containing either  $\Delta$ Np63 $\alpha$  or RRL-MasterMix (+Met) in addition to p53.

To samples assaying the effect different amounts of E6 protein have on the degradation of p53, 5  $\mu$ l 3x assay buffer (+10 mM DTT) was added and the volumes were topped up to 13  $\mu$ l, 13.5  $\mu$ l or 14  $\mu$ l using UP-H<sub>2</sub>O.

*The NaCl concentrations stated are in addition to any ions already present in RRL-MasterMix (+Met).*

Different ion strengths were tested by varying the amount of 3x assay buffer (+10 mM DTT) added to the reactions. The volumes chosen correspond to final NaCl concentrations in the samples of 50, 75, 100 and 150 mM. To achieve these concentrations, 2.5, 3.8, 5 or 7.5  $\mu$ l 3x assay buffer was added to the samples together with UP-H<sub>2</sub>O to top up the volumes to 13  $\mu$ l.

The adjustment of ion strength by adding different amounts of 3x assay buffer containing DTT inevitably adds a second variable that may influence results. To test if small changes in DTT concentration affect the outcome of the degradation assays, samples containing either 0, 1, 3.3 or 5 mM DTT were set up while keeping the amount of NaCl added constant (at 100 mM in the final reaction volume). 3x assay buffer with different DTT concentrations (0 mM, 3 mM, 10 mM and 15 mM) was prepared using DTT (1 M) stock solution. 5  $\mu$ l of 3x assay buffer containing the desired amount of DTT was added to the respective samples and the reaction volume was topped up to 13  $\mu$ l with UP-H<sub>2</sub>O.

The samples were incubated at 25°C for 1 h and afterwards topped up to 15  $\mu$ l by adding 18E6 translation product, followed by another 1 h incubation at 25°C. The degradation reactions were stopped by addition of 17.5  $\mu$ l Urea (10 M) and subsequent incubation at 25°C for 20 min. Then, a mixture of 12.5  $\mu$ l 6x sample buffer and 5  $\mu$ l DTT (1 M) was added to the samples followed by incubation at 25°C for 10 min. The samples were electrophoresed on 12% SDS-PA gels and transferred onto nitrocellulose overnight at 4°C. After protein transfer, the membranes were blocked and subsequently probed for the sample proteins with a mixture of murine DO1 and anti-HA-tag antibodies. Excess antibodies were removed by three washing steps with TBST after which the membranes were incubated with HRP-coupled secondary rabbit anti-mouse antibodies. After three more washing steps with TBST, protein bands were made visible by the use of the ECL system and exposing an X-ray film to the membranes followed by development of the film.

### 2.3.8 Degradation assay with heat shocked p53

Previously, p53 has been found to bind p73 after it was briefly heat shocked at 40°C<sup>52</sup>. The effect of a brief heat shock of p53 on E6 mediated degradation was studied with and without addition of TA- and  $\Delta$ N-isoforms of p63 $\alpha$  and p73 $\alpha$ . The desired proteins (p53, TA- and  $\Delta$ Np63 $\alpha$ , TA- and  $\Delta$ Np73 $\alpha$ , 16E6, and 18E6) were synthesised in vitro as described previously. Synthesis of TA- and  $\Delta$ Np63 $\alpha$  was boosted by addition of KCl and MgAc<sub>2</sub>. The translation products rested on ice while p53 was incubated at 40°C for 15 min. Samples were prepared containing 1  $\mu$ l p53 along with either an isoform of

p63 and p73 (3  $\mu$ l for p63 and  $\Delta$ Np73 $\alpha$ , 1  $\mu$ l for TAp73 $\alpha$ ; degradation samples) or RRL-MasterMix (+Met) solution (p53 negative and positive controls). The total amount of RRL in the samples was normalised to contain the equivalent amount of lysate found in 4  $\mu$ l translation product solutions by adding additional RRL-MasterMix (+Met) where necessary. To all samples, 3  $\mu$ l of 3x assay buffer (+10 mM DTT) was added and the volumes were topped up to 7  $\mu$ l using UP-H<sub>2</sub>O. The samples were incubated at 25°C for 1.5 h, following which 2  $\mu$ l of either 16E6 or 18E6 translation product was added to the degradation samples and 1.6  $\mu$ l together with 0.4  $\mu$ l UP-H<sub>2</sub>O was added to the negative control sample. The samples were incubated at 25°C for 1 h and denatured by addition of 9  $\mu$ l Urea solution (10 M) followed by incubation at 25°C for 20 min. Then, a mixture of 7  $\mu$ l 6x sample buffer and 3  $\mu$ l DTT (1 M) was added to the samples following which they were incubated for 10 min at 25°C. The proteins were separated by SDS-PAGE (12% SDS-PA gel) and transferred onto nitrocellulose overnight at 4°C. The membranes were blocked and probed for the sample proteins with a mixture of murine DO1 and anti-HA-tag antibodies. Excess antibodies were removed by three washing steps with TBST after which the membranes were incubated with HRP-coupled secondary rabbit anti-mouse antibodies. After three more washing steps with TBST, protein bands were revealed using the ECL system and exposing an X-ray film to the membranes followed by development of the film.

### 2.3.9 IVTT of HIF1 $\alpha$ and 18E6 in presence of NOG

Stock solutions of N-Oxalylglycine (NOG) in either HEPES buffer (500 mM, pH 7.4) or UP-H<sub>2</sub>O at final concentrations of 50, 25 and 12.5 mM NOG were prepared from an aqueous master stock at 100 mM. Prior to IVTT, 0.8 vol  $\mu$ l RRL-MasterMix was coincubated with 0.02 vol methionine solution and 0.08 vol of either buffered or unbuffered NOG solutions, HEPES buffer (500 mM, pH 7.4), MG132 (125 or 250  $\mu$ M), DMSO (1:8 dilution in UP-H<sub>2</sub>O) or NF-water at approx. 20-25°C for 30 min. Afterwards, 0.1 vol of either HIF1 $\alpha$  or 18E6 plasmid solution (50 ng/ $\mu$ l) was added to each of the reaction mixtures. The samples were incubated for 1.5 h at 30°C, followed by a.) 30 min on ice and 1 h at 25°C or b.) 2 h at 25°C. Aliquots of the samples were transferred into fresh microcentrifuge tubes, filled up to 10  $\mu$ l with Urea (10 M) and incubated at 25°C for 20 min. Then, 6x sample buffer and DTT (to a final concentration of 10 mM) were both added to the samples followed by another incubation step at 25°C for 10 min. The samples were separated by 8% (HIF1 $\alpha$ ) and 15% (18E6) SDS-PAGE and transferred onto nitrocellulose overnight at 4°C. The membranes were blocked and probed for the sample proteins with anti-HIF1 $\alpha$  or anti-HA-tag (for detection of 18E6) antibodies. Excess antibodies were removed by three washing steps with TBST after which the membranes were incubated with HRP-coupled secondary rabbit anti-mouse antibodies. After three more washing steps with TBST, protein

*The final concentration of HEPES in buffered NOG solutions varied.*

*The final concentration of NOG in the samples was 1, 2 or 4 mM.*

bands were revealed using the ECL system and exposing an X-ray film to the membranes followed by development of the film.

### 2.3.10 Degradation of p53 in presence of NOG

Proteins p53, 16E6 and 18E6 were translated in vitro. The E6 mediated degradation of p53 was assayed in presence of NOG (4 mM) along with positive and negative controls containing no NOG and/or E6. Each of the two experimental set-ups consisted of three reactions with one control sample and two degradation samples that contained either 16E6 or 18E6 in addition to p53.

The E6 proteins and p53 were synthesised in two separate IVTT reactions each, following the previously described protocol. However, instead of 0.08 vol NF-water, 0.08 vol NOG solution (50 mM in HEPES buffer, pH 7.4) was added to one of the two reactions prepared for each protein to achieve a NOG concentration of 4 mM in the final reaction volume. Before plasmid DNA was added, the tubes were incubated for 30 min at RT. Afterwards, plasmids encoding the respective protein of interest were added to the reaction mixtures and the samples were incubated at 30°C for 1.5 h. The translation products were then aliquoted into separate microcentrifuge tubes. Each tube contained 1 µl of p53 (translated in presence or absence of NOG) and 3.2 µl of 3x assay buffer (+10 mM DTT). Additional NOG (50 mM in HEPES, pH 7.4) was added to the three samples containing p53 translated in presence of NOG to keep the concentration of NOG in the total reaction volume of 10 µl constant at 4 mM. The amount of RRL in each sample was equalised to the amount of RRL present in 7 µl translation product by adding more RRL-MasterMix (+Met) to the samples where necessary. The reaction volumes were filled up to 10 µl (control samples) or 7 µl (degradation samples) with UP-H<sub>2</sub>O. The samples were incubated at 25°C for 30 min and then 3 µl of 16E6 or 18E6 was added to the degradation samples. The samples were then incubated at 25°C for 1 h and the reactions were stopped by addition of 10 µl Urea (10 M) followed by incubation at 25°C for 20 min. The samples were further denatured by addition of 7.6 µl 6x sample buffer and 3 µl DTT (1 M) and another incubation step at 25°C for 10 min. The samples were separated by 8% SDS-PAGE and transferred onto nitrocellulose overnight at 4°C. The membranes were blocked and probed for the sample proteins with a mixture of DO1 and anti-HA antibodies. Excess antibodies were removed by three washing steps with TBST after which the membranes were incubated with HRP-coupled secondary rabbit anti-mouse antibodies. After three more washing steps with TBST, protein bands were revealed using the ECL system and exposing an X-ray film to the membranes followed by development of the film.

*Due to the absence of plasmid solution, the NOG concentration was slightly elevated (4.44 mM) during the preincubation step.*

*To samples containing p53, E6 and NOG, only 3 µl 3x assay buffer (+ 10 mM DTT) was added.*

*Note: RRL-MasterMix (+Met) makes up 82% of the IVTT product mixture.*

*The final reaction volume of p53+NOG samples was 9.8 µl.*

### 2.3.11 IVTT of 18E6 at different pH values

Protein 18E6 was translated in vitro at different pH values and in the presence of buffered and unbuffered NOG to see if any of the effects of NOG

seen can be traced back to changes in pH. Prior to the addition of plasmids, 0.8 vol RRL-MasterMix + 0.02 vol methionine was coincubated with 0.08 vol of either citrate buffer (100 mM, pH 4.0-6.0 in increments of 0.5), unbuffered NOG solution (50 mM) or buffered NOG solution (50 mM in 250 mM HEPES, approx. pH 7). Additionally, two more tubes were prepared containing 0.08 vol NF-water along with RRL-MasterMix and methionine to serve as negative and empty vector controls. After an incubation time of 30 min at RT, the plasmid solutions were added and the samples were incubated for 1.5 h at 30°C. The samples were put on ice for 30 min followed by an incubation step for 1 h at 25°C. Aliquots of 3 µl were taken of each sample and mixed with 7 µl Urea (10 M) followed by incubation at 25°C for 20 min. The samples were further denatured by addition of 3.9 µl 6x sample buffer and 1.5 µl DTT (1 M) and incubation at 25°C for 10 min. The samples were separated by 15% SDS-PAGE and transferred onto nitrocellulose overnight at 4°C. The membranes were blocked and probed for the sample proteins with anti-HA antibodies. Excess antibodies were removed by three washing steps with TBST after which the membranes were incubated with HRP-coupled secondary rabbit anti-mouse antibodies. After three more washing steps with TBST, protein bands were revealed using the ECL system and exposing an X-ray film to the membranes followed by development of the film.



## RESULTS

## 3.1 PLASMID AND ION CONCENTRATIONS INFLUENCE YIELD IN IVTT

To find the optimal plasmid concentration to be used in IVTT, different concentrations of plasmids encoding members of the p53 family of proteins as well as E6 proteins from four HPV strains were used in IVTT reactions. The plasmid concentrations tested were 5, 10, 15 or 20 ng/ $\mu$ l. As shown in figure 1, higher plasmid concentrations lead to lower protein yields in all of the observed samples with the exception of TAp73 $\alpha$ . In p73, protein yields are very high even at a plasmid concentration of 20 ng/ $\mu$ l. The only exception to this observation is protein 16E6, of which no bands were detected. The results indicate that the efficiency of in vitro transcription and translation varies with the insert. While p73 gives very strong signals, the two isoforms of p63 (namely  $\Delta$ Np63 $\alpha$  and TAp63 $\alpha$ ) as well as the E6 proteins from HPV strains 5, 8 and 18 give considerably weaker and HPV-16 E6 no signal at all albeit the same antibody was used for the detection of these proteins.

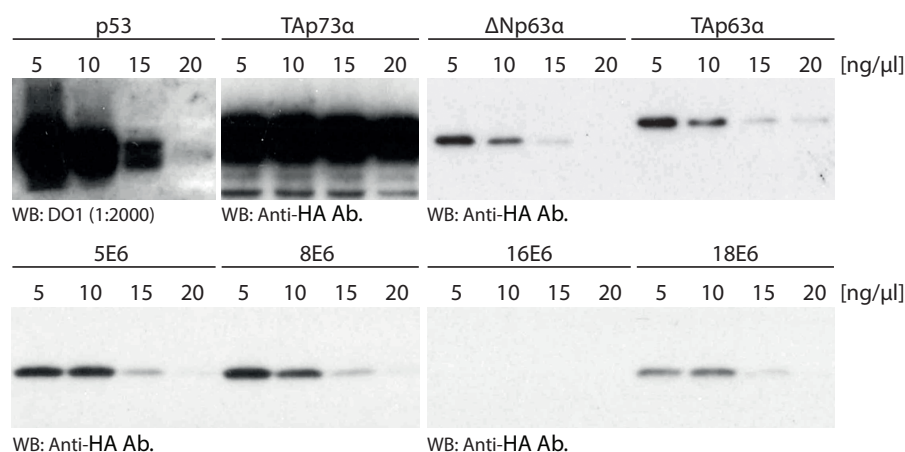


**Figure 1** The effect of plasmid concentration on protein yield in in vitro transcription and translation. The greatest protein yield was achieved with the lowest tested plasmid concentration of 5 ng/ $\mu$ l. However, no bands for 16E6 were found.

The effect of plasmid concentration on protein yield was further studied by varying the plasmid levels in the small range from 3 ng/ $\mu$ l to 7 ng/ $\mu$ l (fig. 2). Similarly to before, the protein yield was higher when the plasmid concentration was lower, giving the strongest band at a plasmid concentration of 3 ng/ $\mu$ l.

Even though the DNA concentration could be optimised to enable the production of detectable amounts of protein in most samples, the discrepancy of protein yields between different plasmids was a problem that had to be overcome. To increase the efficiency at which proteins were produced,

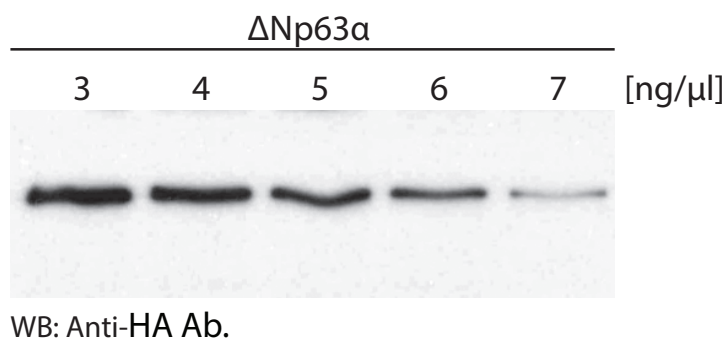


**Figure 2** In continuation of the results shown in figure 1, a plasmid concentration of 3 ng/ $\mu$ l in IVTT yielded more product than higher concentrations of plasmid.

the ion strength in IVTT reactions for  $\Delta$ Np63 $\alpha$  was varied by adding KCl and MgAc<sub>2</sub> at 4 different concentrations. The results shown in figure 3 indicate that increased levels of KCl and MgAc<sub>2</sub> can increase the synthesis of  $\Delta$ Np63 $\alpha$  in vitro considerably up to a certain point (KCl: +0.025 M; MgAc<sub>2</sub>: 0.625 mM) after which the production efficiency decreases. It was found that for  $\Delta$ Np63 $\alpha$ , the optimal IVTT conditions are a plasmid concentration of 3 ng/ $\mu$ l and ion concentrations of +0.05 M, KCl, and 0.625 mM, MgAc<sub>2</sub>.

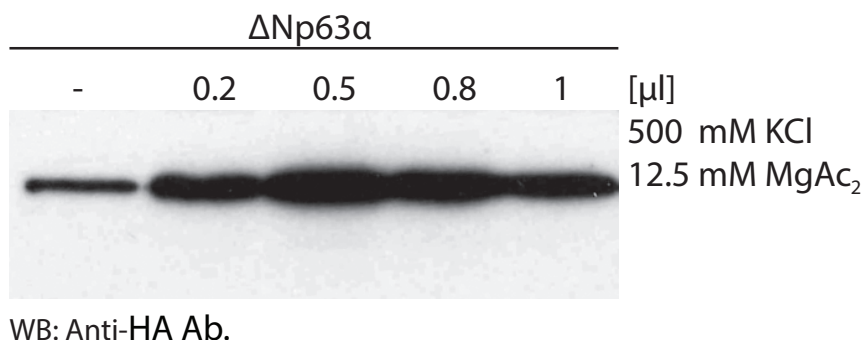


**Figure 3** The effect of ion strength on protein yield in IVTT reactions was studied by adding different amounts (0.2-1  $\mu$ l) of a 500 mM KCl and 12.5 mM MgAc<sub>2</sub> solution. The highest protein yield was achieved by adding 0.5  $\mu$ l ion solution at a final ion concentration of +25 mM KCl and 0.625 mM MgAc<sub>2</sub>.

### 3.2 P63 AND P73 ARE TARGETED FOR DEGRADATION BY HPV-16 E6

In 1990, Scheffner et al. have shown that p53 can be degraded in vitro by E6 proteins of high-risk HPV strains<sup>50</sup>. Similar experiments have been performed by Ben Khalifa et al. in vivo with the TA- and  $\Delta$ N isoforms of p63 $\beta$ , showing that p63 is also susceptible to E6 mediated degradation, though to a lesser extent than p53<sup>20</sup>. Despite being structurally similar to p53<sup>7</sup> and p63<sup>5</sup>, however, E6 mediated degradation of p73 was neither observed in vivo<sup>49</sup>, nor in vitro<sup>47-49</sup>. To confirm these previous findings, degradation assays have been run with high-risk 16E6 and several isoforms of human and murine

p63 and p73 either for 3 h at 25°C (figures 4 and 5, blots A and B) or for 16.5 h at 4°C (blot C) and 25°C (blot D). As shown in figures 4 for p63 and 5 for p73, degradation could be detected in most of the tested isoforms. However, the extent of E6 mediated degradation is weak in comparison to p53 and could therefore rarely be detected in all four assays that have been run.

**TAp63 $\alpha$**  was degraded by 30% as compared to the negative control in experiment A, but this finding could not be reproduced in the other three experiments.

**$\Delta$ Np63 $\alpha$**  was degraded in three of four experiments. The strongest decrease in band intensity occurred in blot D (-80%), whereas no degradation is seen in blot B. Though degradation is evident in blot D, the negative control in this experiment contained less IVTT product solution than the sample. The shown results in this blot are therefore of qualitative nature.

**$\Delta$ Np63 $\beta$**  appears as two bands of which the one with a lower molecular mass is weaker than the other one. The bar plot shown in figure 4 represents the heavier band only. The heavy bands in blots A and C show slight degradation in comparison to the negative control with a weakening of signal intensity by approx. 30%. Barely any difference is seen in the other two blots.

**TAp63 $\gamma$**  and  **$\Delta$ Np63 $\gamma$**  were both translated in vitro from murine genes. In similarity to  **$\Delta$ Np63 $\beta$** , TAp63 $\gamma$  appears as two bands, both of which were used for quantification. In both experiments, a band weakening of approx. 20% has occurred. However, no significant degradation of  **$\Delta$ Np63 $\gamma$**  was found with weakening of signal intensities of 3% and 10% respectively. Despite being of murine origin, these results give a hint that HPV E6 proteins may also target human p63 $\gamma$  for degradation.

The relative band intensities of **TAp73 $\alpha$**  measured following coincubation with 16E6 vary from 0.49 to 0.85. In all of the experiments, a slight reduction in TAp73 $\alpha$  levels was found, indicating that this isoform of p73 can be degraded by 16E6.

**$\Delta$ Np73 $\alpha$**  levels decreased noticeably by 40-50% in blots A, C and D compared to the negative control. In blot B, however, the relative intensity of  **$\Delta$ Np73 $\alpha$**  did not drop by more than 9% and no difference in band intensity can be seen.

**TAp73 $\beta$**  could be degraded by 16E6 in blots A, C and D. The signal intensity in these blots dropped by 20-30% in comparison to the negative controls, whereas the level of TAp73 $\beta$  barely decreased in blot B.

**$\Delta$ Np73 $\beta$**  formed two bands, both of which have been used for quantification of the relative amount of protein present. As shown in blots A, C and D, the remaining protein amounts in these blots lie between 56-82% of the amount present in the negative controls. No degradation was observed in blot D.

**TAp73 $\gamma$**  levels were significantly decreased in blots A-D. While degradation assays that were run for 3 h at 25°C (blots A and B) or overnight at

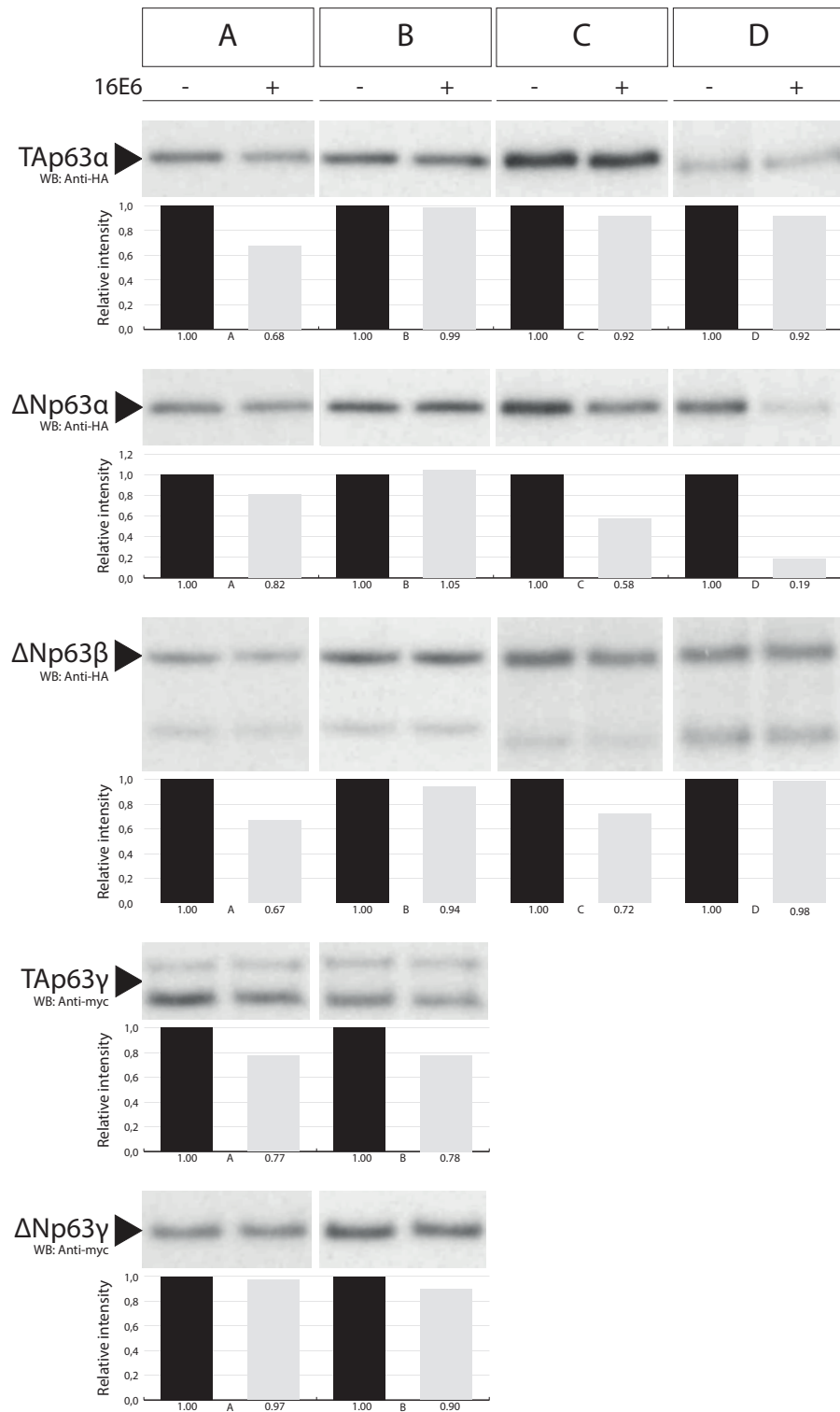


**Figure 4** Degradation of p63 isoforms by HPV-16 E6. The alpha and beta isoforms tested are of human origin, whereas the gamma isoforms are murine p63. The shown samples were incubated with or without 16E6 at 25°C for 3 h (blots A and B) or 16.5 h (blot D) or at 4°C for 16.5 h (blot C). Degradation of p63 mediated by 16E6 seems to be possible, but a lot slower than the degradation of p53.

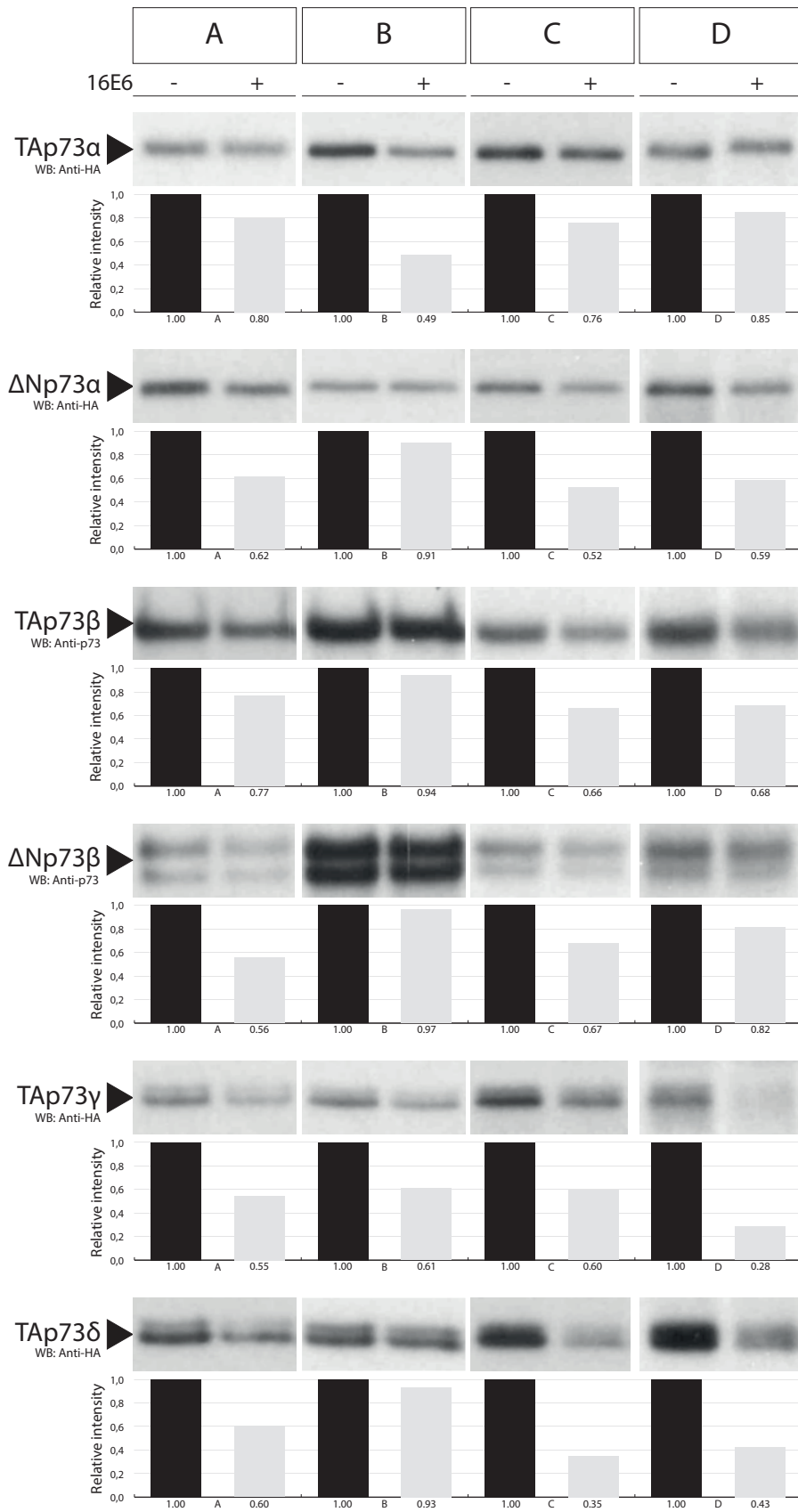


**Figure 5** Degradation of p73 isoforms by HPV-16 E6. The shown samples were incubated with or without 16E6 at 25°C for 3 h (blots A and B) or 16.5 h (blot D) or at 4°C for 16.5 h (blot C). Degradation of p73 mediated by 16E6 was observed for all tested isoforms, though it is weaker than for p53.

4°C (blot C) resulted in a reduction of sample protein by approx. 40%, an overnight coincubation of TAp73 $\gamma$  with 16E6 at 25°C reduced the band intensity by approx. 70% (blot D).

**TAp73 $\delta$**  was efficiently degraded in blots A, C and D, but no significant decrease in band intensity was found in blot B. The reduction of band intensity in blots A, C and D ranges from 65% to 40%.

### 3.3 $\Delta$ NP63 $\alpha$ CAN SLOW DOWN THE DEGRADATION OF P53

Coincubation of p53 with the TA- and  $\Delta$ N-isoforms of p63 $\alpha$  and p73 $\alpha$  did not have a noticeable effect on the E6 mediated degradation of p53, with the exception of  $\Delta$ Np63 $\alpha$  (fig. 6). While p53 was degraded as expected in the presence of the other isoforms tested,  $\Delta$ Np63 $\alpha$  seems to have slowed down the degradation of p53, though it could not prevent it entirely. A difference in degradation efficiency between 16E6 and 18E6 is also evident, as 18E6 could degrade p53 to a lesser extent than 16E6 when  $\Delta$ Np63 $\alpha$  was added to the reaction. This effect was not observed in the other samples. 16E6 was not visibly influenced in fig. 6a, but it was in 6b.

To study the interaction between p53 and  $\Delta$ Np63 $\alpha$  further, a time resolved repetition of this experiment was conducted using 18E6 only. As before, the addition of  $\Delta$ Np63 $\alpha$  seemingly slowed down the reaction (fig. 7a). However, in a second experiment this finding could not be reproduced albeit the amount of  $\Delta$ Np63 $\alpha$  was increased (fig. 7b).

The above stated results could occasionally be reproduced, but not at all times. It was therefore attempted to identify reaction conditions which could influence the results. The concentrations of 18E6, NaCl or DTT were varied to see if the results received would change considerably. The western blot shown in figure 8a tested the effect of different amounts of 18E6, ranging from 1, 1.5 or 2  $\mu$ l translation product added to the reactions. As expected, a higher amount of 18E6 in the reaction slightly speeds up the degradation of p53, but there is no difference between control samples and samples to which  $\Delta$ Np63 $\alpha$  had been added.

To the samples presented in figure 8b, NaCl was added at final concentrations of +50, +75, +100 and +150 mM in addition to any ions already present in the mixtures. The negative control sample contained +100 mM NaCl. As shown in the blot, different concentrations of NaCl did not change the speed of p53 degradation between positive control and  $\Delta$ Np63 $\alpha$  containing samples. However, it appears as if higher NaCl concentrations speed up the degradation process as the bands for p53 in the samples where +150 mM NaCl was added appear to be weaker than the bands of samples containing less NaCl.

The effect of different concentrations of DTT (0, 1, 3.3 or 5 mM DTT) is shown in figure 8c. No difference between p53 positive controls and  $\Delta$ Np63 $\alpha$  containing samples can be seen.

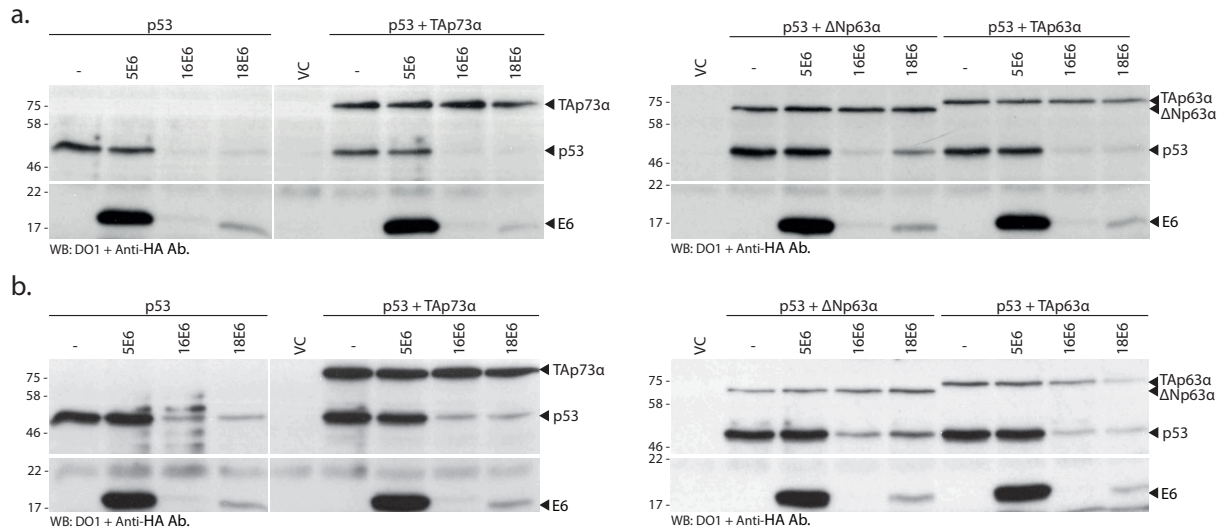


**Figure 6** The influence of p63 and p73 on the degradation of p53. Though TAp63 $\alpha$  and TAp73 $\alpha$  could not influence the results,  $\Delta Np63\alpha$  visibly influenced the degradation of p53. The effect of  $\Delta Np63\alpha$  on p53 is especially prominent with 18E6. The influence of  $\Delta Np63\alpha$  on 16E6 seems to be weaker, but still present as seen in b. However, this effect was not seen in the experiment shown in a.

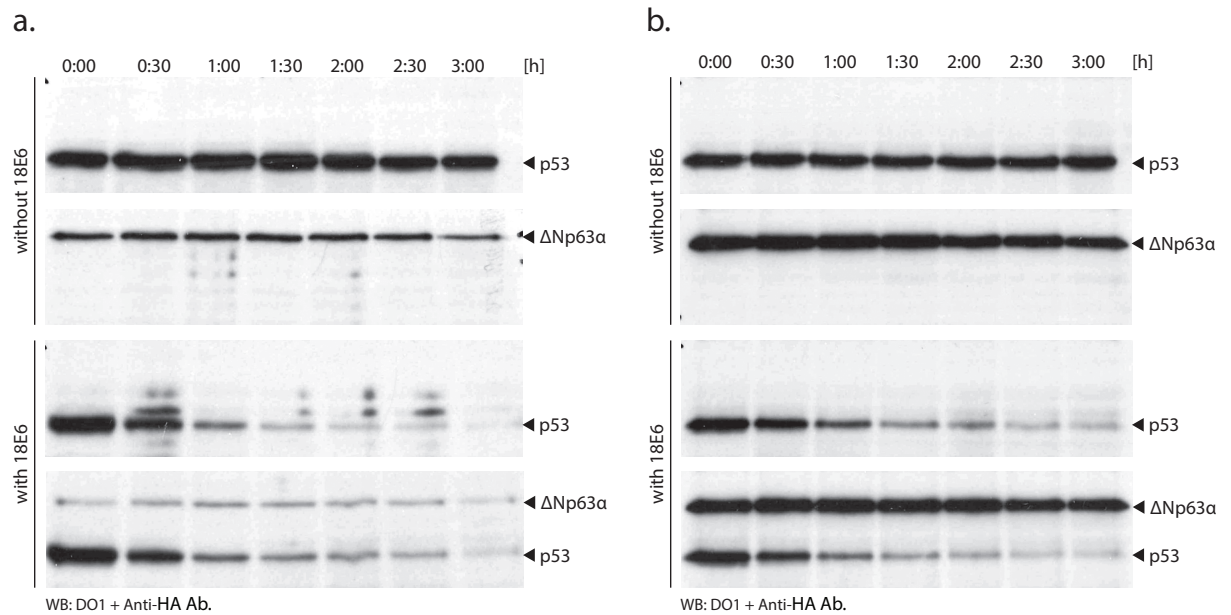
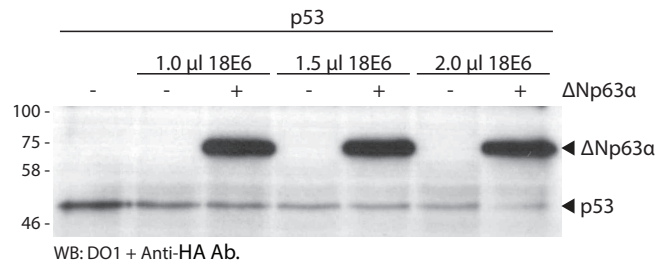
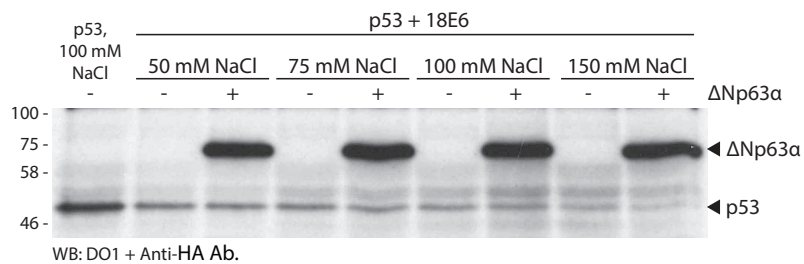


**Figure 7** The process of E6 mediated degradation of p53 was studied over 3 h in steps of 30 min. As shown, there is no degradation of either p53 or  $\Delta Np63\alpha$  without 18E6 present. When  $\Delta Np63\alpha$  was added, the degradation of p53 was slowed down in experiment a., but in experiment b., though more  $\Delta Np63\alpha$  had been added to the reaction, no difference between the control reaction not containing  $\Delta Np63\alpha$  and the reaction containing  $\Delta Np63\alpha$  can be seen.

a.



b.



c.

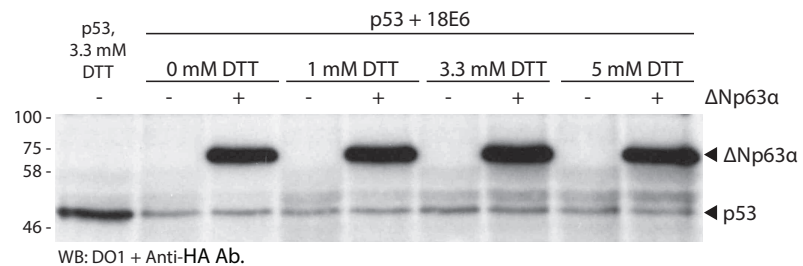


**Figure 8** Degradation assay with p53 at different conditions. (a) Degradation of p53 at varying concentrations of 18E6. The fainter bands for p53 at 2.0 µl 18E6 added as compared to 1.0 µl clearly shows that more E6 correlates with faster degradation. Addition of  $\Delta Np63\alpha$  does not noticeably influence this result. (b.) Degradation of p53 at varying concentrations of NaCl. Reactions with higher concentrations of NaCl give fainter bands for p53. Again, the presence of  $\Delta Np63\alpha$  did not noticeably influence these results. (c) Degradation of p53 at varying concentrations of DTT. At the concentrations tested, neither DTT nor  $\Delta Np63\alpha$  influenced the degradation of p53 and in this way validate the results shown in (b).

### 3.4 HEAT SHOCKED P53 CANNOT BE DEGRADED BY E6

The work of Bensaad et al.<sup>52</sup> suggested a conformational change after which p53 was able to bind to p73. It was tested whether heat shocked p53 could still be degraded by 16E6 and 18E6, and whether p63 or p73 could influence the result. Figure 9 shows clearly that a brief heat shock at 40°C prevents degradation of p53. Addition of p63 and p73 did not change this result. It is,

however, not clear whether this result stems from a conformational change or from complete denaturation of p53.

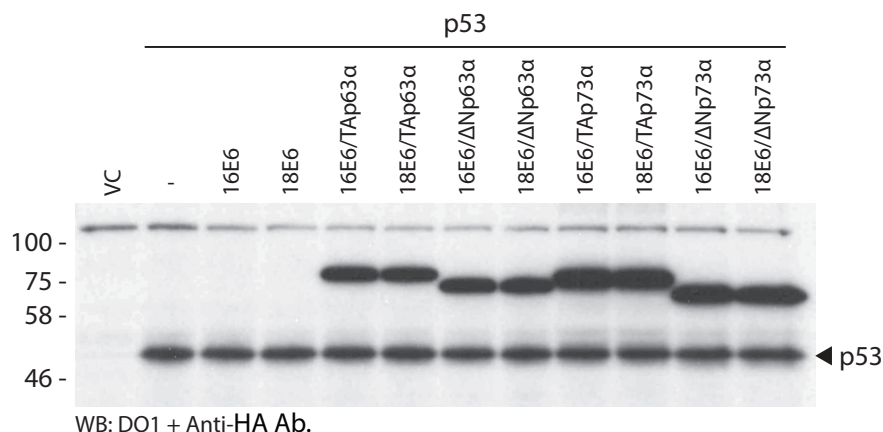


**Figure 9** Degradation assay with heat shocked p53 with or without p63 and p73 isoforms. As a consequence of the brief heat shock, p53 was no longer degraded by 16E6 or 18E6.

### 3.5 N-OXALYLGLYCINE INFLUENCES PROTEIN YIELDS IN IVTT

The 2-oxoglutarate analogue N-Oxalylglycine (NOG) is a competitive inhibitor<sup>53</sup> of 2-oxoglutarate dependent oxygenases such as the PHD hydroxylases, which are involved in the degradation of the HIF1 subunit HIF1 $\alpha$  under normoxia<sup>53</sup>. PHD uses molecular oxygen as a cosubstrate to hydroxylate HIF1 $\alpha$ , which is then ubiquitinated by the E3 ubiquitin ligase complex von Hippel-Lindau<sup>53</sup>. To determine if p53 also needs to be hydroxylated in order for E6 to bind it, p53 was translated in presence of NOG. Because of the acidic nature of NOG, aqueous solutions of it between 12.5-50 mM were found to have a pH of approx. 3-4. When HIF1 $\alpha$  was translated in vitro and subsequently incubated in the presence of HEPES buffered or unbuffered NOG, the detected levels of HIF1 $\alpha$  increased as compared to the respective negative controls (fig. 10). However, HEPES buffered NOG stabilised HIF1 $\alpha$  slightly better at a concentration of 4.0 mM than unbuffered NOG. When compared to reactions that contain the proteasome inhibitor MG132, it appears as if NOG could not fully prevent proteasomal degradation of HIF1 $\alpha$  at the tested concentrations. MG132 was added as an aqueous dilution of DMSO and the respective DMSO control lane yielded a band that is significantly stronger than those seen in the HEPES and water controls. Nevertheless, proof for proteasomal degradation can be seen in additional bands at a size smaller than 46 kDa (see arrow in fig. 10). These bands appear in all of the lanes containing HIF1 $\alpha$  except for those that additionally contain MG132. Remarkably, these bands are a lot stronger in samples that contained unbuffered NOG or DMSO.

A similar experiment conducted with HPV-18 E6 came to a different result (fig. 11a and b). Buffered NOG could barely affect the 18E6 levels with the

only change visible in the sample containing 4 mM NOG, whereas unbuffered NOG lead to a slight increase in the 2 mM and a strong increase in the 4 mM NOG containing samples. The yield of 18E6 in unbuffered NOG was even greater than in the MG132 samples. The amount of 18E6 detected in MG132 samples is comparable to the amount in the 4 mM HEPES buffered NOG sample. Unlike HIF1 $\alpha$ , 18E6 yield was not elevated in the DMSO control sample. The difference between buffered and unbuffered NOG suggests that the increase in 18E6 with higher NOG concentrations may, in fact, be a pH effect. This hypothesis was tested by translating 18E6 *in vitro* at different pH values ranging from pH 4.0-6.0 in increments of 0.5 pH units. However, as shown in figure 11b, no traces of 18E6 could be detected.

When the same experiment was conducted with p53 in a degradation assay, the amount of p53 in the negative control with 4 mM HEPES buffered NOG was significantly larger than in the control sample without NOG (fig. 12). The addition of NOG did not have an effect on the stability of p53 as both, 16E6 and 18E6, could fully degrade p53. This result indicates that p53 does not need to be hydroxylated to be targeted for degradation by E6.

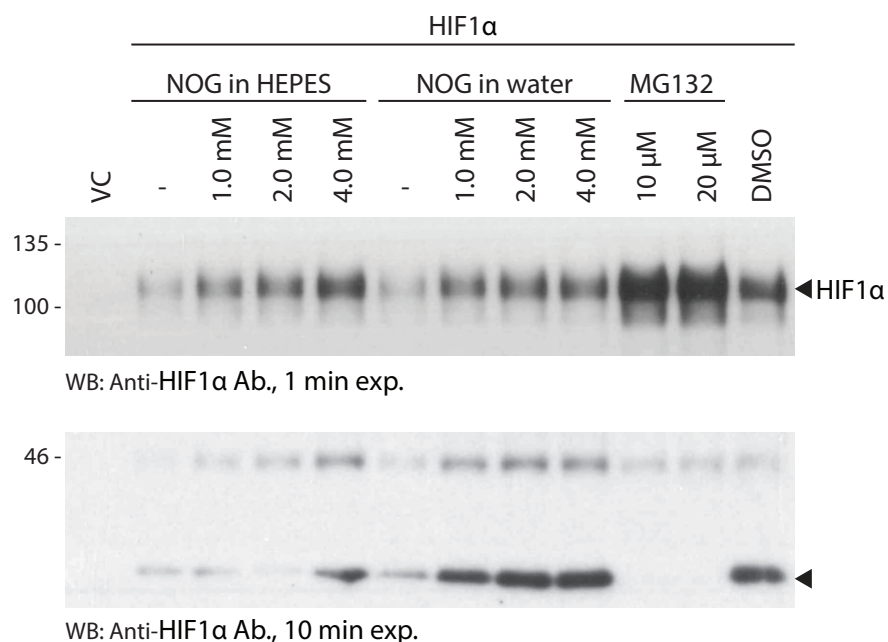


**Figure 10** IVTT of HIF1 $\alpha$  in presence of HEPES buffered NOG, unbuffered NOG or MG132. In both instances, NOG stabilised HIF1 $\alpha$ . Whereas the yield of HIF1 $\alpha$  gradually increases with added pH buffered NOG, barely any difference between the three concentrations of unbuffered NOG in water is noticeable. However, the inhibitory effect of NOG at the concentrations tested still has a weaker effect than the proteasome inhibitor MG132. In all lanes except for the vector control (VC) and the MG132 containing samples, additional bands at a size below 46 kDa are visible. These bands are significantly stronger in lanes containing unbuffered NOG as compared to the bands in lanes where HEPES buffered NOG was used. The absence of these bands in MG132 containing samples suggests that they are degradation fragments of HIF1 $\alpha$ .

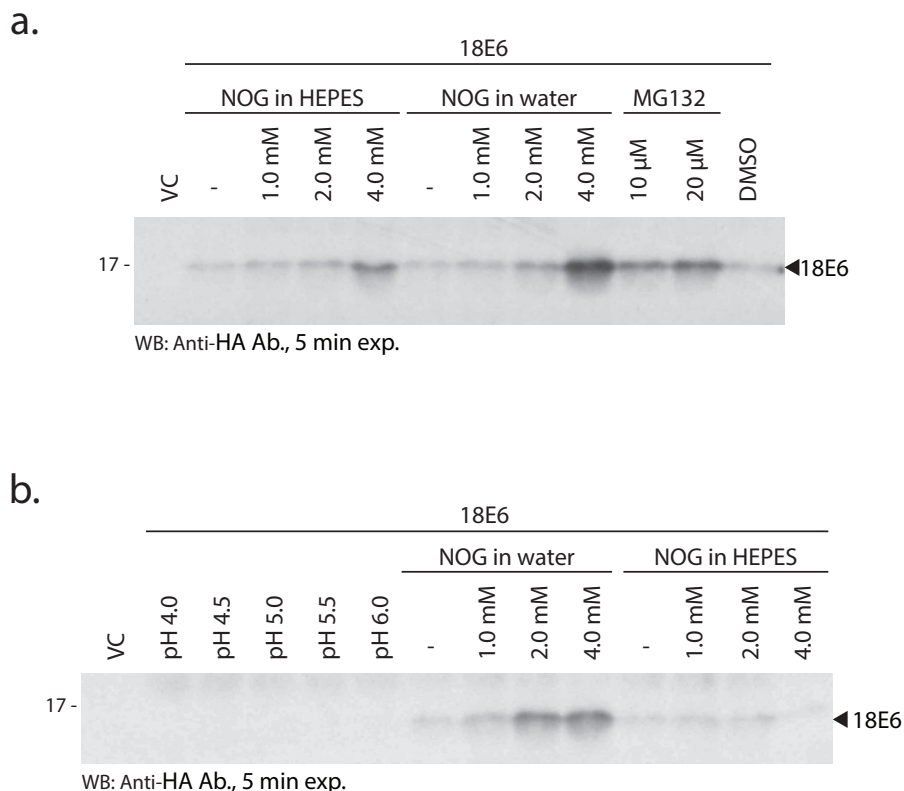


**Figure 11** IVTT of 18E6 in presence of HEPES buffered NOG, unbuffered NOG, MG132 or citrate buffer (pH 4.0-6.0). Reactions containing unbuffered NOG yielded more 18E6 than reactions containing HEPES buffered NOG. As shown in (a), the detected signal for 18E6 in the 4 mM unbuffered NOG containing sample was even greater than the signal of 18E6 in the two samples containing proteasome inhibitor MG132. The assay for IVTT of 18E6 at different pH values in citrate buffer yielded no detectable protein.

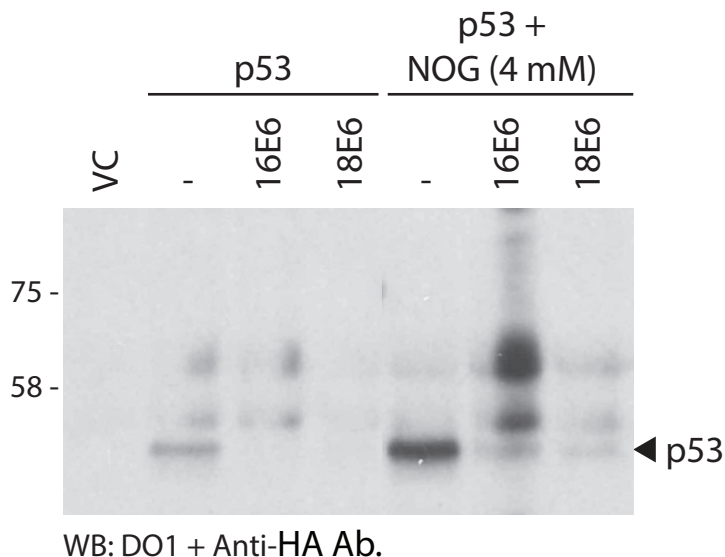


**Figure 12** IVTT and degradation of p53 in presence of pH buffered NOG. In comparison to the negative control without NOG, addition of pH buffered NOG clearly increased protein yields. However, it did not influence the susceptibility of p53 to 16E6 and 18E6.



## DISCUSSION

---

### 4.1 PLASMID AND ION CONCENTRATIONS INFLUENCE YIELD IN IVTT

It was shown that higher proteins yield could be achieved with decreasing plasmid DNA concentrations. High concentrations of plasmids could therefore result in no detectable levels of proteins, going against expectations. Plasmid concentrations of 20 ng/ $\mu$ l, as recommended by the manufacturer, resulted in barely detectable bands for nearly all samples. A possible explanation for this behaviour is that high concentrations of DNA can cause premature termination of translation products, resulting in low amounts of detectable full-length proteins<sup>54</sup>. Another important variable affecting transcription and translation is the concentration of  $Mg^{2+}$  and  $K^+$  in the IVTT mixture. Up to an added concentration of 25 mM KCl and 0.625 mM  $MgAc_2$ , the protein yield increased. At higher ion concentrations, however, it started to decrease. It has been shown that  $Mg^{2+}$  starvation leads to the degradation of ribosomes in *E. coli*<sup>55</sup> while an increase of  $Mg^{2+}$  from 1 mM to 10 mM induces the formation of 70S and 100S ribosome from their respective subunits. Once formed, 70S ribosomes have been found to be stable also at  $Mg^{2+}$  concentrations below 1 mM and up to concentrations of 20 mM, beyond which breakdown was observed<sup>56</sup>. Improved ribosome stability, however, does not guarantee increased protein yields as the optimal  $Mg^{2+}$  concentration for in vitro translation has been found at 1-2 mM<sup>57</sup>.

Similarly to  $Mg^{2+}$ , the absence of  $K^+$  ions can alter the conformation of mammalian ribosome subunits<sup>58</sup>. In contrast to this, high concentrations of  $K^+$  (>100 mM) dissociate the ribosome of *E. coli* in vitro due to competition of monovalent cations with  $Mg^{2+}$  for binding sites on the ribosome<sup>59,60</sup>. Therefore, both, potassium and magnesium in adequate quantities, are necessary for the correct structure and function of ribosomes in vitro.

The different effects of potassium and magnesium on in vitro translation could be seen in figure 3. The maximum protein yield for  $\Delta Np63\alpha$ at +25 mM KCl and +0.625 mM  $MgAc_2$  suggests improved ribosome stability at 30°C. The stated concentrations are in addition to any ions already present in the RRL. The moderate amounts of ions that were added were too low to destabilise the ribosome (compare >100 mM for potassium, >20 mM for magnesium) and improved protein yields significantly. The decrease in protein yields at higher ion concentrations can also be explained with destabilised ribosomes, particularly due to the competition of potassium ions with magnesium. Among the tested plasmids it is noteworthy, that HPV-16 E6 could not be detected regardless of plasmid concentration used or ion concentrations added (data not shown). Other groups have made similar observations that HPV-16 E6, though functional, is difficult to detect in HPV-16 positive

cell lines<sup>61</sup>. Comparison of HPV E6 proteins as shown in figure 1 reveals that E6 proteins incapable of inducing p53 degradation (HPV-5 and -8 E6) appear as stronger bands than those capable of p53 degradation (HPV16 and 18 E6). Consequently, HPV-16 E6 appears to mediate p53 degradation slightly better in some cases than HPV-18 E6 (compare bands for p53 in p53 +  $\Delta$ Np63 $\alpha$  in figure 6). This observation suggests that the difference in band strengths may correlate with the potential of E6 proteins to degrade p53, though other reasons like differing protein yields in IVTT cannot be ruled out.

#### 4.2 P63 AND P73 ARE TARGETED FOR DEGRADATION BY HPV-16 E6

The susceptibility of p53 to proteasomal degradation in the presence of HPV E6 proteins of high-risk strains has been known since the 1990s<sup>50</sup>. With the discovery of the related proteins p63<sup>4</sup> and p73<sup>7</sup>, the question arose whether these homologues of p53 are targeted by E6 for degradation as well. Experiments by Ben Khalifa et al. have shown that the TA- and  $\Delta$ N isoforms of p63 $\beta$  are both susceptible to E6 mediated degradation, though to a lesser extent than p53<sup>20</sup>. The finding that  $\Delta$ Np63 $\beta$  is degraded by HPV-18 E6 could be reproduced in vitro with HPV-16E6 as was shown in figure 4. While the bands in blots A (3h at 25°C) and C (16.5h at 4°C) show a reduction of band intensity by 30%, the bands remained unchanged in blots B (3h at 25°C) and D (16.5h at 25°C). Ben Khalifa et al. have achieved a reduction of  $\Delta$ Np63 $\beta$  levels by approx. 65% in HeLa cells after 2h of cycloheximide treatment<sup>20</sup>. The in relative terms stronger degradation of  $\Delta$ Np63 $\beta$  may be a consequence of the more protected environment inside the cells as compared to RRL. The compositions of RRL and HeLa cell cytoplasm differ and as experimental conditions were not identical, results may vary. However, the reason why degradation of  $\Delta$ Np63 $\beta$  did not occur in blots B and D is not known. The proteins used in blots C and D came from the same batch with the only difference being the incubation temperature. Considering the successful degradation of  $\Delta$ Np63 $\beta$  at 25°C in blot A, the higher incubation temperature used for the sample in blot D as compared to blot C does not necessarily explain this result. Repetition of this experiment in cells may give more reproducible results.

The results for TA- and  $\Delta$ Np63 $\alpha$  are similar to the results of  $\Delta$ Np63 $\beta$ . TAp63 $\alpha$  showed susceptibility to degradation in only one case, and  $\Delta$ Np63 $\alpha$  in three cases. It is important to point out that the control band for  $\Delta$ Np63 $\alpha$  in blot D contained less IVTT product solution than the degradation band. Nevertheless, the remarkable reduction in band strength by approx. 80% at 25°C for 16.5 h is the strongest reduction measured. Degradation was less efficient at 4°C for 16.5 h which can be explained by the low temperature. It is possible that the higher rate of degradation at 25°C in blot D (16.5 h incubation) as compared to blots A and B (3 h each) is due to the much longer incubation time. However, similarly to  $\Delta$ Np63 $\beta$  this does not explain why no degradation was observed in blot B. Stability issues with the proteins involved are likely reasons. TAp63 $\gamma$  and  $\Delta$ Np63 $\gamma$  were both of murine origin

and could still slightly be degraded by HPV E6 proteins. It is therefore likely, that the human counterparts are susceptible to E6 mediated degradation as well.

Of the isoforms of p73 that were tested (TAp73 $\alpha$ , - $\beta$ , - $\gamma$  and - $\delta$ ;  $\Delta$ Np73 $\alpha$  and - $\beta$ ), degradation occurred in at least two of the four experiments conducted for each isoform. These results contradict the observations made by other groups who have conducted degradation experiments with p73 (isoforms p73  $\alpha$  and  $\beta$  of unspecified N-terminus) and have neither seen degradation *in vivo*<sup>49</sup>, nor *in vitro*<sup>47-49</sup>. As seen with p63, the tested isoforms of p73 could not be degraded in all cases. However, though the degradation is a lot weaker than for p53, the results presented in figure 5 confirm that, contradicting previous reports, p73 can be degraded by E6. In previous work it has been demonstrated that, unlike p53, the degradation of TAp63 $\beta$  does not depend on E6AP<sup>20</sup>. It remains to be elucidated whether this is also the case for p73.

The degradation of p53 by E6 as described by Scheffner et al. results in the functional inactivation of p53<sup>50</sup>, thereby promoting the progression of a cell towards malignancy. Due to the many different isoforms of p63 and p73 with, in part, opposing functions, their role in tumorigenesis is very complex. While isoforms with a full-length transactivation domain are usually required for efficient expression of target genes, the truncated  $\Delta$ N isoforms can act as suppressors of transactivation by TAp63/73 or p53<sup>5,62</sup>. Essentially, the TA isoforms can be considered as tumour suppressors, whereas the  $\Delta$ N isoforms appear to be oncogenes. The ratio of TA/ $\Delta$ N isoforms could have a greater impact on the net effect of the expressed isoforms than the absolute amounts present. The degradation of p63 and p73 could shift this ratio and thereby potentially influence the behaviour of the cell without having to be as efficient as the degradation of p53. With the present data, no statements regarding the direction of the ratio shift can be made owing to the large variation of degradation efficiency among the conducted experiments. In human cervical tissue,  $\Delta$ Np63 $\alpha$  was found to be the most commonly expressed isoform of p63<sup>5,26</sup>. Interestingly, the strongest result with a reduction of -80% *in vitro* was obtained for this isoform. As was shown in figure 4, the most impressive results were obtained after a 16.5 h incubation at 25°C. In contrast to this, the degradation of TAp63 $\alpha$  was found to be weaker with remaining relative intensities of 68-92%. In healthy cervical epithelia, TAp63 was not found to be expressed at detectable levels whereas expression of TAp63 was detectable in the cervical carcinoma cell line ME180<sup>5</sup>. This implies that TAp63 may play a role in the progression of cervical cancer and the degradation of  $\Delta$ Np63 $\alpha$ , which under normal circumstances can suppress the transcriptional activities of TAp63, may enhance the role of TAp63 in tumorigenesis. Though the conditions inside the cell differ, these results along with the observation of reduced  $\Delta$ Np63 $\alpha$  expression in increasingly dedifferentiated tumour cells indicate that E6 mediated degradation of  $\Delta$ Np63 $\alpha$  may play a role in the carcinogenesis of cervical cancer.

Unlike described by several research groups in the past<sup>47–49</sup>, p73 was found to be susceptible to E6 mediated degradation in vitro. As for p63, the degradation efficiency was modest for most of the isoforms, though reductions down to approx. 30% were achieved for TAp73 $\gamma$  and TAp73 $\delta$ . Among the isoforms of p73, TAp73 $\gamma$  is considered to be especially similar to p53 in structure and function which may be an explanation why this isoform seems to be more susceptible to degradation than the other isoforms tested<sup>63–66</sup>.

In most cases, p73 is only weakly or not detectable in human cervixes<sup>67</sup>. The absence of p73 in cervical cancers is associated with radioresistance whereas radiosensitive cervical cancers show increased expression of p73<sup>67</sup>. Though the reduction of p73 levels by E6 could in theory contribute to radioresistance, no correlation between HPV infection and p73 expression has been found and so these findings speak against a role of p73 degradation in cancer<sup>67</sup>.

Furthermore, as the absence of both p63 and p73 is known to inhibit apoptosis, a slight reduction of both proteins could therefore potentially have an influence on the survival of HPV infected cells. However, no correlation between HPV infection and p73 expression was previously found and the influence of E6 mediated degradation of p73 in the development and progression of cervical cancer remains questionable.

The structural similarity of p63 and p73 to p53 might explain why isoforms of both proteins can be degraded to some extent in vitro. As the degradation of p53 was found to be a lot quicker than the degradation of p63 and p73 it is possible that in the presence of all three proteins the degradation of p63 and p73 would be even slower or not occur at all. The coincubation of p53 with one of the isoforms of p63 or p73, however, was indeed shown to influence the degradation kinetics in some experiments (see section 3.3). Whether or not the degradation of p63 and p73 can have an influence on the cell remains to be elucidated. The artificial conditions in an in vitro setting differ from the situation within cells in respect of the concentrations of involved proteins and the components and structures present inside the cell. Further experiments are needed to understand if this observation does play a noticeable role in infected cells.

#### 4.3 $\Delta$ Np63 $\alpha$ CAN SLOW DOWN THE DEGRADATION OF P53

The observation that  $\Delta$ Np63 $\alpha$  can influence the pace at which p53 is degraded agrees with the result that  $\Delta$ Np63 $\alpha$  is among the most efficiently degraded isoforms of p63 in vitro. As Ben Khalifa et al have shown, TAp63 $\beta$  can be co-precipitated along with E6<sup>20</sup> and it is likely that the same may also be true for  $\Delta$ Np63 $\alpha$ . The observed effect was more prominent in samples containing 18E6 than in those containing 16E6. Considering that the binding affinity of 16E6 to p53 is higher than the affinity of 18E6 to p53<sup>68</sup>, p53 may therefore also be more efficiently degraded by 16E6. By binding E6,  $\Delta$ Np63 $\alpha$  might reduce the amount of E6 available to degrade p53 and in this way simulate a lower E6 concentration. In figure 8a, the influence of changes in 18E6

concentration has been shown to small but measurable and may therefore be a plausible explanation. If the affinity of E6 for  $\Delta\text{Np63}\alpha$  is higher than its affinity for any of the other tested variants of p63 and p73, this would explain why only  $\Delta\text{Np63}\alpha$  has been found to influence the degradation kinetics of p53. On the other hand, no decrease in  $\Delta\text{Np63}\alpha$  band strength was observed in presence of p53.

The results showing an influence of  $\Delta\text{Np63}\alpha$  on the degradation kinetics of p53 are notoriously difficult to reproduce. This has been illustrated in the time resolved experiment seen in figure 7, where a slowed down degradation is seen in blot (a), but not in blot (b). The experimental conditions in (b) were the same as in (a), but with a higher concentration of  $\Delta\text{Np63}\alpha$  in the degradation assay that has been achieved by adding less plasmid DNA and additional KCl and  $\text{MgAc}_2$  to the IVTT reaction. Though experiments have revealed that the concentrations of E6 and NaCl influence the degradation kinetics in general, no conditions have been found that ease the reproduction of the described effect. The same problem has also lead to great variations in the measured degradation of p63 and p73 isoforms mediated by E6. In the case of  $\Delta\text{Np63}\alpha$ , the measured degradation ranges from 0% to 80% (see section 3.2). Due to the rapid degradation of p53, larger quantities of p53 may be required to better resolve the influence of  $\Delta\text{Np63}\alpha$ . The sole increase of  $\Delta\text{Np63}\alpha$  concentrations has not been found to have a detectable effect (data not shown). Given the difficulty of reproducing the interference of  $\Delta\text{Np63}\alpha$  with the degradation of p53, it remains questionable if this can be reproduced in cells where the conditions such as oxygen concentration, redox potential etc. differ from those in RRL.

#### 4.4 HEAT SHOCKED P53 CANNOT BE DEGRADED BY E6

A study conducted by Hansen et al demonstrated that p53 is thermally unstable and quickly loses its ability to bind DNA after 10 minutes of incubation at 37°C<sup>69</sup>. Furthermore, Bensaad et al have described that a brief heat shock of p53 at 40°C induces a conformational change that allows it to bind to p73<sup>52</sup>. The inability of 16E6 and 18E6 to degrade heat shocked p53 may be due to the described conformational change or possibly full denaturation of p53. It is unclear if E6 can bind to heat shocked p53 at all and if heat treated p53 can still carry out any of its tumour suppressive functions.

#### 4.5 N-OXALYLGLYCINE INFLUENCES PROTEIN YIELDS IN IVTT

N-oxalylglycine (NOG) is a molecular mimic of 2-oxoglutarate (2OG) and a competitive inhibitor of 2OG-dependent oxygenases such as prolyl hydroxylase domain-containing oxygenases (PHDs)<sup>53,70</sup>. Under normoxic conditions, PHDs use molecular oxygen along with 2OG to hydroxylate conserved proline residues on the oxygen sensor Hypoxia-inducible factor (HIF), which is composed of the regulatory subunit HIF1 $\alpha$  and the constitutive subunit HIF1 $\beta$ <sup>53,70,71</sup>. The E3 ubiquitin ligase complex von Hippel-Lindau

then binds HIF1 $\alpha$ , ubiquitinates it and thereby promotes its proteasomal degradation<sup>72</sup>. As such, the levels of in vitro translated HIF1 $\alpha$  detected in western blots gradually increased the more pH buffered NOG was added. However, there was a difference between HEPES buffered NOG and unbuffered NOG that resulted in the accumulation of fragments of HIF1 $\alpha$  at a size between 32-46 kDa. This fragment was detected in all of the samples except for those that contained the proteasome inhibitor MG132, suggesting that it is a result of proteasomal degradation. Among the samples where this fragment was detected, it is noteworthy that the strongest bands were detected in samples containing unbuffered NOG or DMSO. Considering the similarity of the HEPES control to the aqueous control, it is unlikely that HEPES itself is responsible for this behaviour. If the fragments and the detected full-length HIF1 $\alpha$  were put together, one would find that a lot more HIF1 $\alpha$  had been produced in unbuffered NOG containing samples. The same observation was also made when the experiment was repeated with 18E6, where HEPES buffered NOG containing samples contained less 18E6 than those containing unbuffered NOG. Unbuffered NOG may have had a positive influence on the IVTT efficiency, but the added amounts of NOG were not sufficient to stabilise all of the produced moieties. DMSO had a similar effect with HIF1 $\alpha$ , but this observation was not reproducible with 18E6. IVTT assays with MG132 and unbuffered NOG together could give further clues to understand the underlying mechanism.

As mentioned above, IVTT reactions for 18E6 containing unbuffered NOG yielded a stronger band for 18E6 in western blots than IVTT reactions with added pH buffered NOG, HEPES buffer or water. Possible reasons are improved IVTT efficiency or increased stability of E6 at the applied conditions (e.g. possibly reduced pH due to NOG). A negative influence of HEPES itself can be excluded as there is no difference between the water and the HEPES control samples. Bands from 18E6 translated in presence of the proteasome inhibitor MG132 were weaker than those from 18E6 translated in unbuffered NOG, supporting the hypothesis of increased protein production in presence of unbuffered NOG. The DMSO control sample for 18E6 is comparable to the other control samples in HEPES buffer or water. Translation of 18E6 in pH buffered NOG yielded similar amounts as 18E6 translated in presence of MG132. The influence of pH on 18E6 protein yields was tested by adding citrate buffer to the IVTT reactions. Citrate buffer was chosen for its broad pH range (approx. pH 3.0 - 6.0) as it combines the pH of unbuffered NOG stock solutions (approx. 3.0 - 4.0) with near neutral values. Nevertheless, no bands were detected in samples to which citrate buffer was added. The most concentrated NOG stock solution contained 50 mM NOG whereas the buffers had a molarity of 100 mM. The lower concentration of NOG may have led to a less dramatic pH drop in IVTT reactions than the buffers or may not have significantly affected the pH value at all. Measurement of the pH value of IVTT reaction mixtures was not possible due to the small volumes and the strong red colour of RRL. As the low pH values or citric acid itself may have interfered with the IVTT reactions, the experiment should be repeated

with a different buffer system exploring the pH range between 6.0-8.0 in more detail. Furthermore, to ensure HEPES does not decrease the efficiency of IVTT reactions, experiments containing different amounts of HEPES at near neutral pH values (pH approx. 7.4) are needed.

When pH buffered NOG was added to IVTT reactions, the protein yield of p53 as detected in western blots was significantly higher than in control reactions free of NOG. In this regard, p53 behaves similarly to HIF1 $\alpha$  although no experiments with unbuffered NOG and p53 have been conducted. The variant of p53 used in this experiment encodes proline at codon 72. Though p53-72R is known to be more susceptible to E6 mediated degradation<sup>73</sup>, p53-72P was degraded efficiently regardless of whether pH buffered NOG had been added or not. p53 is known to be hydroxylated on a lysine residue located at position 382 by the 2OG-dependent oxygenase Jumonji domain-containing 6 (JMJD6)<sup>74</sup>. However, JMJD6 was not found to affect the stability of p53<sup>74</sup> and therefore does not explain the elevated amounts of p53 produced in the presence of pH buffered NOG. Deschoemaeker et al suggest that p53 may also be hydroxylated by PHD1, which, unlike JMJD6, hydroxylates proline residues<sup>75</sup>. In this case, the amount of p53 produced in presence of pH buffered NOG could potentially differ between the two variants encoding either arginine or proline at position 72. To be able to distinguish which 2OG-dependent oxygenases are responsible for this behaviour, specific inhibitors could be used. The experiment should also be repeated with p53-72R to see if the effect of pH buffered NOG on protein yield is limited to p53-72P or if it is generally observed in p53. As reviewed by Markolovic et al, there is evidence for the involvement of several 2OG-dependent oxygenases in the regulation of the cellular translation machinery<sup>76</sup>. It is possible that the increase of p53 yields is a consequence of suppressed hydroxylation of parts of the translation machinery. This may in part also explain the results obtained for HIF1 $\alpha$  and 18E6.



SUMMARY AND CONCLUSION

---

In this thesis it was shown that all tested members of the p53 family can be degraded to some extent in the presence of high-risk type HPV E6. The degradation of p63 and p73 is a lot less efficient than in p53, and the extent varies a lot depending on the experimental conditions. Because of this, no definite statement regarding the differences in susceptibility of the isoforms tested can be made. Nevertheless, the present results challenge previous findings claiming that p73 is not degraded by E6<sup>47-49</sup>.

Given the homology of the p53 family members<sup>4,5,7</sup> it is not surprising that E6 can also target p63 and p73 for degradation. Assuming that p53 is the main target of E6, p63 and p73 may only bind weakly to E6, therefore explaining the low degradation efficiency measured. This was illustrated when  $\Delta$ Np63 $\alpha$  had been added to p53 degradation assays as it could, in some experiments, slow down the degradation of p53 while staying seemingly unaffected. A possible explanation is the reduction of freely available E6 to degrade p53. However, a higher affinity of E6 to p53 also implies that high levels of p53 may interfere with the degradation of p63/p73. On the other hand, the physiological degradation of p53 in healthy, unstressed cells combined with the rapid degradation of p53 by E6 may still allow for the degradation of p63 and p73 to take place inside the cell.

As a consequence of the slight degradation of p63 and p73 isoforms, the ratio of TA to  $\Delta$ N isoforms may be shifted and thereby influence the net function of both proteins. The measured degradation *in vitro* is too weak to fully deplete p63 or p73, but it may be strong enough to shift the TA/ $\Delta$ N ratio towards a more oncogenic state. Cell culture experiments are needed to gain more insights into the extent of p63 and p73 degradation and its consequences in HPV infected cells. In addition, further *in vitro* studies are needed to establish an improved protocol for the degradation of p63 and p73.

Heat shocking p53 at 40°C prevents E6 mediated degradation. However, it cannot be excluded that E6 can still bind to heat shocked p53 and immunoprecipitation experiments may give further insights. In either case, a study conducted by Hansen et al. has shown that heat shocked p53 quickly loses its ability to bind to DNA following incubation at 40°C or higher<sup>69</sup>. It is likely that a brief heat shock inactivates p53 permanently and a previously discovered interaction between heat shocked p53 and p73 was not found to trigger degradation of p53 in presence of E6<sup>52</sup>.

NOG as a 2-oxoglutarate analogue that can act as an inhibitor of 2OG-dependent oxygenases has remarkable effects when it is added to IVTT reactions. When p53 was synthesised *in vitro* in the presence of pH buffered NOG, the protein yield was significantly higher than in reactions lacking NOG. As reviewed by Markolovic et al, 2OG-dependent oxygenases are involved in many cellular processes and they are likely to cause the increase of

p53 levels in IVTT as well<sup>76</sup>. More experiments are required to understand if this result is limited to p53 with a proline at position 72, or if this behaviour can generally be observed in p53. Though an involvement of the translation machinery itself cannot be excluded, it remains to be elucidated why this effect has not been seen to the same extent in HPV E6. p53 was still degraded in presence of NOG, which means that hydroxylation of p53 is not required for binding of E6.

HPV-18E6 is seemingly stabilised or more efficiently produced in vitro when non-pH buffered NOG was added to the reaction mixture. In contrast, pH buffered NOG barely or only weakly affected E6 levels. Though this suggests an influence of pH on the stability or translation efficiency of 18E6, no bands for 18E6 were seen in western blots when citrate buffer in the pH range from 4.0-6.0 had been added to the reaction mixtures. It is possible that unbuffered NOG only slightly influences the pH of the reaction mixture, or that citrate interferes with IVTT. The stark increase of HIF1 $\alpha$  fragments when unbuffered NOG had been added to the reactions suggests that another plausible explanation is an increase in translation efficiency along with improved proteasomal degradation. However, further experiments are needed to understand the role of NOG in IVTT.

## BIBLIOGRAPHY

---

1. Meek D. W. Tumour suppression by p53: a role for the DNA damage response? *Nature Reviews Cancer* **9**, 714–723 (2009).
2. Evans D. G. R. & Ingham S. L. Reduced life expectancy seen in hereditary diseases which predispose to early-onset tumors. *The application of clinical genetics* **6**, 53 (2013).
3. Polager S. & Ginsberg D. p53 and E2f: partners in life and death. *Nature Reviews Cancer* **9**, 738–748 (2009).
4. Schmale H. & Bamberger C. A novel protein with strong homology to the tumor suppressor p53. *Oncogene* **15**, 1363–1367 (1997).
5. Yang A., Kaghad M., Wang Y., Gillett E., Fleming M. D., Dötsch V., Andrews N. C., Caput D. & McKeon F. p63, a p53 homolog at 3q27–29, encodes multiple products with transactivating, death-inducing, and dominant-negative activities. *Molecular cell* **2**, 305–316 (1998).
6. Osada M. *et al.* Cloning and functional analysis of human p51, which structurally and functionally resembles p53. *Nature Medicine* **4**, 839–843 (1998).
7. Kaghad M. *et al.* Monoallelically Expressed Gene Related to p53 at 1p36, a Region Frequently Deleted in Neuroblastoma and Other Human Cancers. *Cell* **90**, 809–819 (1997).
8. Ferraiuolo M., Di Agostino S., Blandino G. & Strano S. Oncogenic Intra-p53 family member interactions in human cancers. *Frontiers in oncology* **6** (2016).
9. Khoury M. P. & Bourdon J.-C. p53 Isoforms An Intracellular Microprocessor? *Genes & cancer* **2**, 453–465 (2011).
10. Marcel V., Perrier S., Aoubala M., Ageorges S., Groves M. J., Diot A., Fernandes K., Tauro S. & Bourdon J.-C.  $\Delta$ 160p53 is a novel N-terminal p53 isoform encoded by  $\Delta$ 133p53 transcript. *FEBS letters* **584**, 4463–4468 (2010).
11. Beyer U., Moll-Rocek J., Moll U. M. & Döbelstein M. Endogenous retrovirus drives hitherto unknown proapoptotic p63 isoforms in the male germ line of humans and great apes. *Proceedings of the National Academy of Sciences* **108**, 3624–3629 (2011).
12. Su X., Chakravarti D. & Flores E. R. p63 steps into the limelight: crucial roles in the suppression of tumorigenesis and metastasis. *Nature Reviews Cancer* **13**, 136–143 (2013).
13. Murray-Zmijewski F., Lane D. & Bourdon J. p53/p63/p73 isoforms: an orchestra of isoforms to harmonise cell differentiation and response to stress. *Cell Death & Differentiation* **13**, 962–972 (2006).

14. Di Como C. J., Urist M. J., Babayan I., Drobnjak M., Hedvat C. V., Teruya-Feldstein J., Pohar K., Hoos A. & Cordon-Cardo C. p63 expression profiles in human normal and tumor tissues. *Clinical Cancer Research* **8**, 494–501 (2002).
15. DiRenzo J., Signoretti S., Nakamura N., Rivera-Gonzalez R., Sellers W., Loda M. & Brown M. Growth factor requirements and basal phenotype of an immortalized mammary epithelial cell line. *Cancer research* **62**, 89–98 (2002).
16. Nylander K., Vojtesek B., Nenutil R., Lindgren B., Roos G., Zhanxiang W., Sjöström B., Dahlqvist Å. & Coates P. J. Differential expression of p63 isoforms in normal tissues and neoplastic cells. *The Journal of pathology* **198**, 417–427 (2002).
17. Vanbokhoven H., Melino G., Candi E. & Declercq W. p63, a story of mice and men. *Journal of Investigative Dermatology* **131**, 1196–1207 (2011).
18. Koster M. I., Kim S., Mills A. A., DeMayo F. J. & Roop D. R. p63 is the molecular switch for initiation of an epithelial stratification program. *Genes & development* **18**, 126–131 (2004).
19. Jacobs W. B., Govoni G., Ho D., Atwal J. K., Barnabe-Heider F., Keyes W. M., Mills A. A., Miller F. D. & Kaplan D. R. p63 is an essential proapoptotic protein during neural development. *Neuron* **48**, 743–756 (2005).
20. Ben Khalifa Y., Teissier S., Tan M.-K. M., Phan Q. T., Daynac M., Wong W. Q. & Thierry F. The Human Papillomavirus E6 Oncogene Represses a Cell Adhesion Pathway and Disrupts Focal Adhesion through Degradation of TAp63 $\beta$  upon Transformation. *PLoS Pathog* **7**, 1–15 (2011).
21. Petitjean A., Ruptier C., Tribollet V., Hautefeuille A., Chardon F., Cavard C., Puisieux A., Hainaut P. & de Fromental C. C. Properties of the six isoforms of p63: p53-like regulation in response to genotoxic stress and cross talk with  $\Delta$ Np73. *Carcinogenesis* **29**, 273–281 (2008).
22. Amelio I., Grespi F., Annicchiarico-Petruzzelli M. & Melino G. p63 the guardian of human reproduction. *Cell cycle* **11**, 4545–4551 (2012).
23. Dohn M., Zhang S. & Chen X. p63 $\alpha$  and  $\Delta$ Np63 $\alpha$  can induce cell cycle arrest and apoptosis and differentially regulate p53 target genes. *Oncogene* **20**, 3193 (2001).
24. Helton E. S., Zhu J. & Chen X. The unique NH<sub>2</sub>-terminally deleted ( $\Delta$ N) residues, the PXXP motif, and the PPXY motif are required for the transcriptional activity of the  $\Delta$ N variant of p63. *Journal of Biological Chemistry* **281**, 2533–2542 (2006).
25. Stefansson I. M., Salvesen H. B. & Akslen L. A. Loss of p63 and cytokeratin 5/6 expression is associated with more aggressive tumors in endometrial carcinoma patients. *International journal of cancer* **118**, 1227–1233 (2006).

26. Zhou Y., Xu Q., Ling B., Xiao W. & Liu P. Reduced expression of  $\Delta\text{Np}63\alpha$  in cervical squamous cell carcinoma. *Clinical & Investigative Medicine* **34**, 184–191 (2011).
27. Urist M. J., Di Como C. J., Lu M.-L., Charytonowicz E., Verbel D., Crum C. P., Ince T. A., McKeon F. D. & Cordon-Cardo C. Loss of p63 expression is associated with tumor progression in bladder cancer. *The American journal of pathology* **161**, 1199–1206 (2002).
28. Puig P., Capodieci P., Drobnjak M., Verbel D., Prives C., Cordon-Cardo C. & Di Como C. J. p73 Expression in Human Normal and Tumor Tissues. *Clinical Cancer Research* **9**, 5642–5651 (2003).
29. Grob T., Novak U., Maisse C., Barcaroli D., Lüthi A., Pirnia F., Hügli B., Graber H., De Laurenzi V., Fey M. *et al.* Human  $\Delta\text{Np}73$  regulates a dominant negative feedback loop for TAp73 and p53. *Cell death and differentiation* **8**, 1213 (2001).
30. Allocati N., Di Ilio C. & De Laurenzi V. p63/p73 in the control of cell cycle and cell death. *Experimental cell research* **318**, 1285–1290 (2012).
31. Rufini A., Agostini M., Grespi F., Tomasini R., Sayan B. S., Niklison-Chirou M. V., Conforti F., Velletri T., Mastino A., Mak T. W. *et al.* p73 in Cancer. *Genes & cancer* **2**, 491–502 (2011).
32. Müller M., Schilling T., Sayan A., Kairat A., Lorenz K., Schulze-Bergkamen H., Oren M., Koch A., Tannapfel A., Stremmel W. *et al.* TAp73/ $\Delta\text{Np}73$  influences apoptotic response, chemosensitivity and prognosis in hepatocellular carcinoma. *Cell Death & Differentiation* **12**, 1564–1577 (2005).
33. Jost C. A., Jr W. G. K. & Marin M. C. p73 is a human p53-related protein that can induce apoptosis. *Nature* **389**, 191–194 (Nov. 1997).
34. Liu G., Nozell S., Xiao H. & Chen X.  $\Delta\text{Np}73\beta$  is active in transactivation and growth suppression. *Molecular and cellular biology* **24**, 487–501 (2004).
35. Flores E. R., Tsai K. Y., Crowley D., Sengupta S., Yang A., Mckeon F. & Jacks T. p63 and p73 are required for p53-dependent apoptosis in response to DNA damage. *Nature* **416**, 560–564 (Apr. 2002).
36. Strano S., Munarriz E., Rossi M., Cristofanelli B., Shaul Y., Castagnoli L., Levine A. J., Sacchi A., Cesareni G., Oren M. *et al.* Physical and functional interaction between p53 mutants and different isoforms of p73. *Journal of Biological Chemistry* **275**, 29503–29512 (2000).
37. Yim E.-K. & Park J.-S. The role of HPV E6 and E7 oncoproteins in HPV-associated cervical carcinogenesis. *Cancer Research and Treatment* **37**, 319–324 (2005).
38. Carter J. R., Ding Z. & Rose B. R. HPV infection and cervical disease: a review. *Australian and New Zealand Journal of Obstetrics and Gynaecology* **51**, 103–108 (2011).

39. Münger K., Baldwin A., Edwards K. M., Hayakawa H., Nguyen C. L., Owens M., Grace M. & Huh K. Mechanisms of human papillomavirus-induced oncogenesis. *Journal of virology* **78**, 11451–11460 (2004).
40. Stubenrauch F. & Laimins L. A. *Human papillomavirus life cycle: active and latent phases* in *Seminars in cancer biology* **9** (1999), 379–386.
41. Adams A. K., Wise-Draper T. M. & Wells S. I. Human papillomavirus induced transformation in cervical and head and neck cancers. *Cancers* **6**, 1793–1820 (2014).
42. Huibregtse J. M., Scheffner M. & Howley P. M. Cloning and expression of the cDNA for E6-AP, a protein that mediates the interaction of the human papillomavirus E6 oncoprotein with p53. *Molecular and cellular biology* **13**, 775–784 (1993).
43. Goodrich D. W., Wang N. P., Qian Y.-W., Eva Y.-H. L. & Lee W.-H. The retinoblastoma gene product regulates progression through the G1 phase of the cell cycle. *Cell* **67**, 293–302 (1991).
44. Hawley-Nelson P., Vousden K. H., Hubbert N. L., Lowy D. R. & Schiller J. T. HPV16 E6 and E7 proteins cooperate to immortalize human foreskin keratinocytes. *The EMBO journal* **8**, 3905 (1989).
45. Bosch F., Lorincz A., Munoz N., Meijer C. & Shah K. The causal relation between human papillomavirus and cervical cancer. *Journal of clinical pathology* **55**, 244–265 (2002).
46. Bellanger S., Tan C. L., Xue Y. Z., Teissier S. & Thierry F. Tumor suppressor or oncogene? A critical role of the human papillomavirus (HPV) E2 protein in cervical cancer progression. *Am J Cancer Res* **1**, 373–389 (2011).
47. Marin M. C., Jost C. A., Irwin M. S., DeCaprio J. A., Caput D. & Kaelin W. G. Viral Oncoproteins Discriminate between p53 and the p53 Homolog p73. *Molecular and Cellular Biology* **18**, 6316–6324 (1998).
48. Bálint E., Bates S. & Vousden K. H. Mdm2 binds p73 $\alpha$  without targeting degradation. *Oncogene* **18**, 3923–3929 (1999).
49. Park J.-S., Kim E.-J., Lee J.-Y., Sin H.-S., Namkoong S.-E. & Um S.-J. Functional inactivation of p73, a homolog of p53 tumor suppressor protein, by human papillomavirus E6 proteins. *International Journal of Cancer* **91**, 822–827. ISSN: 1097-0215 (2001).
50. Scheffner M., Werness B. A., Huibregtse J. M., Levine A. J. & Howley P. M. The E6 oncoprotein encoded by human papillomavirus types 16 and 18 promotes the degradation of p53. *Cell* **63**, 1129–1136 (1990).
51. Sambrook J. & Russell D. *Molecular Cloning: A Laboratory Manual* 3rd ed. (Cold Spring Harbor Laboratory Press, 2001).
52. Bensaad K., Le Bras M., Unsal K., Strano S., Blandino G., Tominaga O., Rouillard D. & Soussi T. Change of Conformation of the DNA-binding Domain of p53 Is the Only Key Element for Binding of and Interference with p73. *Journal of Biological Chemistry* **278**, 10546–10555 (2003).

53. Jaakkola P. *et al.* Targeting of HIF- $\alpha$  to the von Hippel-Lindau Ubiquitylation Complex by O<sub>2</sub>-Regulated Prolyl Hydroxylation. *Science* **292**, 468–472 (2001).
54. Craig D., Howell M. T., Gibbs C. L., Hunt T. & Jackson R. J. Plasmid cDNA-directed protein synthesis in a coupled eukaryotic in vitro transcription-translation system. *Nucleic acids research* **20**, 4987–4995 (1992).
55. Mccarthy B. The effects of magnesium starvation on the ribosome content of Escherichia coli. *Biochimica et Biophysica Acta* **55**, 880–889 (1962).
56. Tissières A., Watson J., Schlessinger D. & Hollingworth B. Ribonucleo-protein particles from Escherichia coli. *Journal of Molecular Biology* **1**, 221–233 (1959).
57. Shenvi C. L. Accessibility of 18S rRNA in human 40S subunits and 80S ribosomes at physiological magnesium ion concentrations—implications for the study of ribosome dynamics. *Rna* **11**, 1898–1908 (Jan. 2005).
58. Näslund P. & Hultin T. Structural and functional defects in mammalian ribosomes after potassium deficiency. *Biochimica et Biophysica Acta (BBA) - Nucleic Acids and Protein Synthesis* **254**, 104–116 (1971).
59. Zitomer R. S. & Flaks J. G. Magnesium dependence and equilibrium of the Escherichia coli ribosomal subunit association. *Journal of Molecular Biology* **71**, 263–279 (1972).
60. Klein D. J. The contribution of metal ions to the structural stability of the large ribosomal subunit. *RNA* **10**, 1366–1379 (Jan. 2004).
61. Ajiro M. & Zheng Z.-M. E6<sup>E7</sup>, a Novel Splice Isoform Protein of Human Papillomavirus 16, Stabilizes Viral E6 and E7 Oncoproteins via HSP90 and GRP78. *mBio* **6** (2015).
62. Zaika A. I., Slade N., Erster S. H., Sansome C., Joseph T. W., Pearl M., Chalas E. & Moll U. M.  $\Delta$ Np73, a dominant-negative inhibitor of wild-type p53 and TAp73, is up-regulated in human tumors. *The Journal of experimental medicine* **196**, 765–780 (2002).
63. Moll U. M. & Slade N. p63 and p73: Roles in Development and Tumor Formation. *Molecular cancer research* **2**, 371–386 (2004).
64. Vilgelm A., El-Rifai W. & Zaika A. Therapeutic prospects for p73 and p63: rising from the shadow of p53. *Drug Resistance Updates* **11**, 152–163 (2008).
65. Momii Y., Izumi H., Shiota M., Onitsuka T., Abe T., Kobayashi H., Miyamoto N., Uchiumi T. & Kohno K. p73 $\gamma$  transactivates the p21 promoter through preferential interaction with the p300/CBP-associated factor in human prostate cancer cells. *Oncology Reports* (Jan. 2007).
66. Sauer M., Bretz A. C., Beinoraviciute-Kellner R., Beitzinger M., Burek C., Rosenwald A., Harms G. S. & Stiewe T. C-terminal diversity within the p53 family accounts for differences in DNA binding and transcriptional activity. *Nucleic acids research* **36**, 1900–1912 (2008).

67. Si Liu S., Leung R. C.-Y., Chan K. Y.-K., Chiu P.-M., Cheung A. N.-Y., Tam K.-F., Ng T.-Y., Wong L.-C. & Ngan H. Y.-S. p73 expression is associated with the cellular radiosensitivity in cervical cancer after radiotherapy. *Clinical cancer research* **10**, 3309–3316 (2004).
68. Lechner M. S. & Laimins L. A. Inhibition of p53 DNA binding by human papillomavirus E6 proteins. *Journal of virology* **68**, 4262–4273 (1994).
69. Hansen S., Hupp T. R. & Lane D. P. Allosteric regulation of the thermostability and DNA binding activity of human p53 by specific interacting proteins. *Journal of Biological Chemistry* **271**, 3917–3924 (1996).
70. Fraisl P., Aragonés J. & Carmeliet P. Inhibition of oxygen sensors as a therapeutic strategy for ischaemic and inflammatory disease. *Nature Reviews Drug Discovery* **8**, 139–152 (2009).
71. Epstein A. C. *et al.* C. elegans EGL-9 and Mammalian Homologs Define a Family of Dioxygenases that Regulate HIF by Prolyl Hydroxylation. *Cell* **107**, 43–54 (2001).
72. Ohh M., Park C. W., Ivan M., Hoffman M. A., Kim T.-Y., Huang L. E., Pavletich N., Chau V. & Kaelin W. G. Ubiquitination of hypoxia-inducible factor requires direct binding to the  $\beta$ -domain of the von Hippel–Lindau protein. *Nature cell biology* **2**, 423–427 (2000).
73. Whibley C., Pharoah P. D. & Hollstein M. p53 polymorphisms: cancer implications. *Nature Reviews Cancer* **9**, 95–107 (2009).
74. Wang F., He L., Huangyang P., Liang J., Si W., Yan R., Han X., Liu S., Gui B., Li W. *et al.* JMJD6 promotes colon carcinogenesis through negative regulation of p53 by hydroxylation. *PLoS Biol* **12**, e1001819 (2014).
75. Deschoemaeker S., Di Conza G., Lilla S., Martín-Pérez R., Mennerich D., Boon L., Hendrikx S., Maddocks O. D., Marx C., Radhakrishnan P. *et al.* PHD1 regulates p53-mediated colorectal cancer chemoresistance. *EMBO molecular medicine*, e201505492 (2015).
76. Markolovic S., Wilkins S. E. & Schofield C. J. Protein hydroxylation catalyzed by 2-oxoglutarate-dependent oxygenases. *Journal of Biological Chemistry* **290**, 20712–20722 (2015).

## DECLARATION

---

I hereby swear that I have compiled this work without external help or the use of sources and aides other than those permitted. Ideas and concepts taken from unpublished sources, published literature or the internet have been indicated by precise source citations.

This work has not been submitted in the same or similar form to any other examiners as a form of assessment. I am aware that offenders may be punished ('use of unauthorised assistance') and that further legal action may ensue.

*Vienna, April 2017*

---

Michael T. Pinner



#### COLOPHON

This document was typeset using the typographical look-and-feel `classicthesis` developed by André Miede. The style was inspired by Robert Bringhurst’s seminal book on typography “*The Elements of Typographic Style*”. `classicthesis` is available for both  $\text{\LaTeX}$  and  $\text{\LyX}$ :

<https://bitbucket.org/amiede/classicthesis/>

*Final Version* as of 4th April 2017 (`classicthesis`).